

EPA-600/2-75-023

August 1975

Environmental Protection Technology Series

**ABSORPTION
OF SULFUR DIOXIDE IN SPRAY COLUMN
AND TURBULENT CONTACTING
ABSORBERS**

U.S. Environmental Protection Agency
Office of Research and Development
Washington, D. C. 20460

ABSORPTION OF SULFUR DIOXIDE IN SPRAY COLUMN AND TURBULENT CONTACTING ABSORBERS

by

C. Y. Wen and L. S. Fan

Department of Chemical Engineering
West Virginia University
Morgantown, West Virginia 26506

Grant No. R-800781
ROAP No. 21ACY-041
Program Element No. 1AB013

EPA Project Officer: Robert H. Borgwardt

Industrial Environmental Research Laboratory
Office of Energy, Minerals, and Industry
Research Triangle Park, North Carolina 27711

Prepared for

U. S. ENVIRONMENTAL PROTECTION AGENCY
Office of Research and Development
Washington, D. C. 20460

August 1975

EPA REVIEW NOTICE

This report has been reviewed by the National Environmental Research Center - Research Triangle Park, Office of Research and Development, EPA, and approved for publication. Approval does not signify that the contents necessarily reflect the views and policies of the Environmental Protection Agency, nor does mention of trade names or commercial products constitute endorsement or recommendation for use.

RESEARCH REPORTING SERIES

Research reports of the Office of Research and Development, U.S. Environmental Protection Agency, have been grouped into series. These broad categories were established to facilitate further development and application of environmental technology. Elimination of traditional grouping was consciously planned to foster technology transfer and maximum interface in related fields. These series are:

1. ENVIRONMENTAL HEALTH EFFECTS RESEARCH
2. ENVIRONMENTAL PROTECTION TECHNOLOGY
3. ECOLOGICAL RESEARCH
4. ENVIRONMENTAL MONITORING
5. SOCIOECONOMIC ENVIRONMENTAL STUDIES
6. SCIENTIFIC AND TECHNICAL ASSESSMENT REPORTS
9. MISCELLANEOUS

This report has been assigned to the ENVIRONMENTAL PROTECTION TECHNOLOGY series. This series describes research performed to develop and demonstrate instrumentation, equipment and methodology to repair or prevent environmental degradation from point and non-point sources of pollution. This work provides the new or improved technology required for the control and treatment of pollution sources to meet environmental quality standards.

This document is available to the public for sale through the National Technical Information Service, Springfield, Virginia 22161.

Publication No. EPA-600/2-75-023

Table of Contents

	Page
List of Figures	v
List of Tables	viii
 Chapter	
1. Introduction	1
1.1 Description of Scrubber-Holding Tank Recycle System Using Limestone/Lime Slurries	2
1.2 Scope of Investigation	2
2. Literature Review	6
2.1 General Review of Gas-Liquid Contactors . .	6
2.2 Review of Turbulent Contacting Absorbers . .	6
2.3 Review of the Chemistry of SO ₂ Scrubbing Using Limestone/Lime Slurries	21
2.3.1 Chemical Reaction in SO ₂ Absorption	21
2.3.2 Oxidation and Solid Precipitation . .	23
3. Mathematical Model for SO ₂ Absorption in Spray and TCA Scrubbers	25
3.1 Introduction	25
3.2 Mathematical Models of Spray and TCA Scrubbers	25
3.2.1 Scrubber Model	27
3.2.2 Mass Transfer Coefficients	34
3.2.3 Effect of Magnesium on SO ₂ Scrubbing Efficiency	54

Table of Contents (Continued)

	Page
3.3 Simulation of SO ₂ Scrubbing With Limestone and Lime Slurries	58
4. Mechanism of SO ₂ Scrubbing With Limestone Slurries	65
4.1 Introduction	65
4.2 Reaction Mechanism	66
5. Analysis of pH for Lime Slurry at the Outlet of the Scrubber	76
5.1 Introduction	76
5.2 Liquid Phase Material Balance for the Scrubber	77
6. Conclusion and Discussion	86
Nomenclature	90
Bibliography	94
Appendices	
A. Numerical Example of the Simulation of EPA/RTP TCA Scrubber Using Lime Slurry as the Scrubbing Medium	99
B. Some Comments on the Concentration of Reactant, C _B , Calculated Via Equilibrium Computer Program	104

List of Figures

Figure	Page
1.1 Configuration of Scrubber-Holding Tank Recycle System Using Limestone/Lime Slurries as the Scrubbing Medium	3
3.1 Schematic of TVA Shawnee Three-Bed TCA	28
3.2 Schematic of TVA Shawnee Spray Tower	29
3.3 Schematic of the EPA/RTP Research TCA Scrubber	30
3.4 Ratio of the Mass Transfer Resistances for Spray Devices, R_s , as a Function of the pH of the Scrubbing Slurry at the Inlet of the Scrubber	37
3.5 An Idealized Stage of a Turbulent Contacting Absorber	42
3.6 Typical Operating Data for the TVA Shawnee TCA Showing the Dependence of the SO_2 Removal Efficiency on the Inlet SO_2 Concentration	46
3.7 The Ratio of the Gas Film to the Liquid Film Mass Transfer Resistance as a Function of the Inlet SO_2 Partial Pressure for the TVA Shawnee TCA	48
3.8 The Pre-Exponential Function, A_s , in the Expression for R , the Ratio of Resistances, as a Function of the pH of the Inlet Slurry for the TVA Shawnee TCA Without Spheres and Spray Column. Low Magnesium Concentration (Mg < 350 ppm)	50
3.9 The Pre-Exponential Function, A_p , in the Expression for R , the Ratio of Resistances, as a Function of the pH of the Inlet Slurry for the Packed Section of TVA TCA and EPA TCA. Low Magnesium Concentration (Mg < 350 ppm)	53
3.10 The Effect of Magnesium in the Scrubbing Slurry on the Ratio of the Gas to Liquid Mass Transfer Resistances in the Spray Section	55

List of Figures (Continued)

Figure	Page
3.11 The Effect of Magnesium in the Scrubbing Slurry on the Ratio of the Gas to Liquid Mass Transfer Resistances in the Packed Section	56
3.12 Comparison of the Predicted and Observed SO ₂ Removal Efficiencies for Spray-Type Devices Using Limestone Slurry as the Scrubbing Medium	60
3.13 Comparison of the Predicted and Observed SO ₂ Removal Efficiencies for TCA Scrubbers Using Limestone Slurry as Scrubbing Medium	61
3.14 Comparison of the Predicted and Observed SO ₂ Removal Efficiencies for TCA Scrubber Using Lime Slurry as the Scrubbing Medium	62
4.1 The Overall Ratio of the Mass Transfer Resistances as a Function of the Arithmetic Average of the SO ₂ Partial Pressure in the Bulk Gas Phase Plotted as Suggested by Equation (4-6). Data from the TVA Shawnee TCA. Low Magnesium Concentration in the Limestone Slurry	68
4.2 The Overall Ratio of Mass Transfer Resistance as a Function of the Arithmetic Average of the SO ₂ Partial Pressure in the Bulk Gas Phase Plotted as Suggested by Equation (4-6). Data from the TVA Shawnee TCA. High Magnesium Concentration in the Limestone Slurry	70
4.3 Idealization of the Concentration Profiles of Species Important in the Transfer of SO ₂ Across the Gas-Liquid Interface and the Chemical Reaction in the Liquid Phase	73
4.4 The Overall Ratio of Mass Transfer Resistances as a Function of the Arithmetic Average of the SO ₂ Partial Pressure in the Bulk Gas Phase Plotted as Suggested by Equation (4-6). Data from the TVA Shawnee Spray Column. Low Magnesium Concentration in the Limestone Slurry	74

List of Figures (Continued)

		Page
Figure		
5.1	Comparison of the Predicted and Observed Values of η for Lime Slurry at the Inlet and Outlet of EPA/RTP TCA Scrubber	81
5.2	Comparison of the Predicted and Observed Outlet Slurry pH for the Simulation of EPA/RTP TCA Scrubber Using Lime Slurry as the Scrubbing Medium	84
5.3	Comparison of the Predicted and Observed SO ₂ Removal Efficiencies for the Simulation of EPA/RTP TCA Scrubber Using Lime Slurry as the Scrubbing Medium	86
A.1	Relationship Between η and pH for Lime Scrubbing System for the Example Given in Appendix B	102

List of Tables

Table	Page
2.1 Classification of Gas-Liquid Contactors	7
2.2 Characteristics of Gas-Liquid Contactors	8
2.3 Data on Sulfur Dioxide Reduction Using Gas-Liquid Contactors	12
3.1 Range of Data for the Spray Column and TCA Operating Without Packing Spheres Used in Constructing Figure 3.4	38
3.2 Range of Data for the EPA/RTP Research TCA Scrubber Used in the Estimation of the Gas Side Mass Transfer Coefficient for the Packed Section of the TCA Scrubber	44
3.3 Range of Data for the TVA Shawnee TCA and EPA In-House TCA Used in Determining A_p in Figure 3.9	52
3.4 Range of Scrubber Operating Data Used in Calculating the Effect of Magnesium on the Pre-Exponential Factor, A	57
3.5 Summary of Equations Necessary for Simulating the Performance of the TVA Shawnee TCA and Spray Column and the EPA In-House TCA	59
3.6 Range of Data Used in Constructing Figure 3.14. Data is for the EPA In-House TCA Using Lime Slurries as the Scrubbing Medium	63
4.1 Comparison Between the Calculated Concentration of the Species Which is Hypothesized to Instanta- neously and Irreversibly React With Absorbed SO_2 as H_2SO_3 in Limestone Slurries and Selected Species Concentration Predicted from Equilibrium . . .	71
5.1 Range of Data Used in Constructing Figures 5.1, 5.2 and 5.3. Data is for the EPA In-House TCA Using Lime Slurries as the Scrubbing Medium	84
A.1 Operating Conditions and Reference for the Example Given in Appendix B. Data is for the EPA In-House TCA Using Lime Slurries as the Scrubbing Medium	104

Chapter 1

Introduction

The presence of sulfur dioxide in flue gases occurs in many common processes such as the combustion of heavy oil and coal, smelting operations, sulfuric acid manufacture and metallurgical processes. Because of the current concern over impending energy shortages fuels with high sulfur content will be increasingly used as important sources of energy in the future. As a result, the environmental aspects of the burning of high sulfur fuel and its associated SO₂ emission problems are being given considerable attention by governments throughout the world.

Due to the EPA regulations on sulfur dioxide emissions associated with stack gas, much effort has gone into studying the removal of sulfur dioxide from these gases. Several processes for the removal of sulfur dioxide from stack gases have been proposed and studied in both small and large scale pilot-plant operations. One of these processes is the wet scrubbing process which utilizes recycled limestone or lime slurries as scrubbing liquid. It is this process upon which the attention of this study is focused

In this chapter, a general description of the wet scrubbing processes which utilize limestone/lime slurries as the scrubbing medium is given and the scope of the study is defined.

1.1 Description of Scrubber-Holding Tank Recycle System Using Limestone/Lime Slurries

A simplified flow sheet for a wet scrubber-holding tank recycle system is given in Figure 1.1. The absorption of sulfur dioxide is carried out in the scrubber where intimate contact between the upward flowing gas and downward flowing slurry is maintained. The holding tank plays an important role in the recycle system by providing sufficient holding time for the scrubber effluent so that the precipitation of calcium sulfite and calcium sulfate which are produced by the reaction of sulfur dioxide and oxygen with limestone or lime slurries will take place. These precipitants are then purged from the system through the clarifier. It is in the make-up tank that fresh limestone/lime slurries are provided for the slurry recycle system.

Two of the most promising scrubbers for carrying out the sulfur dioxide scrubbing with limestone/lime slurries appear to be the turbulent contacting absorber (TCA) and spray tower. Several large scale scrubber-holding tank recycle systems utilizing these scrubbers have been built and a number of research projects on wet scrubber systems have been sponsored by the EPA to test the performance and reliability of these scrubbers.

1.2 Scope of Investigation

In this study, a mathematical model is developed which describes the absorption of sulfur dioxide by limestone or lime slurries in a scrubber. Parameters appearing in this model are evaluated from

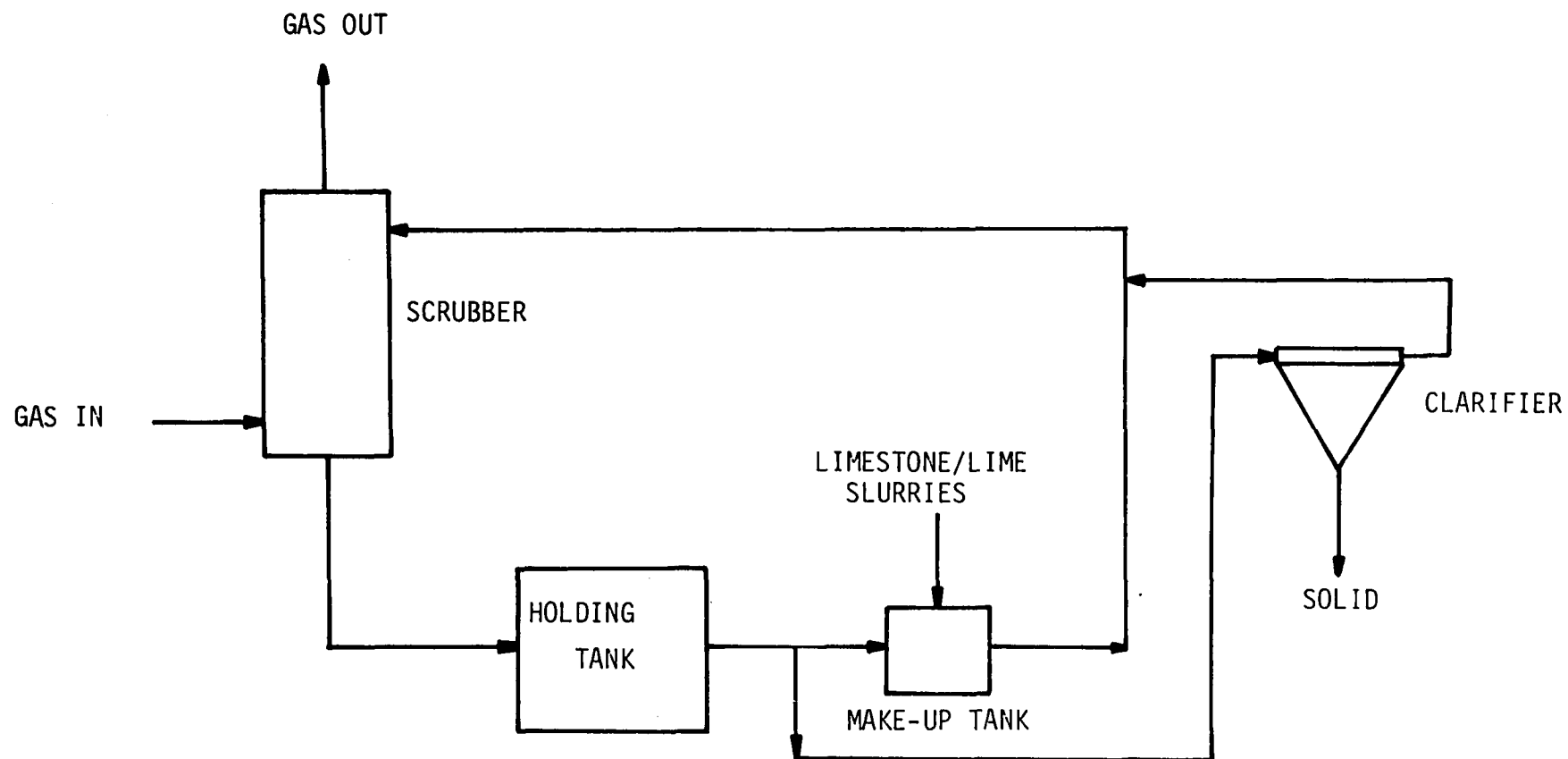


Figure 1.1 Configuration of Scrubber-Holding Tank Recycle System Using Limestone/Lime Slurries as the Scrubbing Medium.

experimental data obtained from the large scale turbulent contacting absorber located at the TVA Shawnee power station and the EPA in-house turbulent contacting absorber and spray column at Research Triangle Park, North Carolina. Correlations are developed for the gas film mass transfer coefficients and the overall coefficients in the liquid film based on the hydrodynamic and chemical characteristics of the system.

The scrubbing of sulfur dioxide from flue gas is simulated utilizing the correlations developed in this study for the gas film mass transfer coefficient and the ratio of mass transfer resistances. The results are compared with the experimentally observed sulfur dioxide removal efficiencies for widely differing size TCA scrubbers and spray column scrubbers. It is demonstrated that the mathematical model developed here can be used in the design and scale-up of the process of absorbing SO_2 into limestone or lime slurries in spray column and TCA scrubbers.

In light of the mathematical model and correlations developed in this study the complex mechanism of SO_2 absorption into the scrubbing slurry is analyzed and the key liquid phase reactions are identified.

The rate of CO_2 transfer between the gas and liquid phases in the scrubber effluent is also studied. Since the kinetics of precipitation and dissolution of the calcium salts found in wet scrubber processes are uncertain at this stage, the differential material balances for the liquid phase in the scrubber cannot be

solved. However, calculations based on assuming chemical equilibrium in the liquid phase are shown to approximate the liquid phase analysis reasonably accurately.

Chapter 2

Literature Review

2.1 General Review of Gas-Liquid Contactors

Gas-liquid contactors can be classified according to the geometry of dispersed fluid, the relative direction of flow of two phases, the type of operation, and the force utilized. A detailed description of such classification has been shown in Table 2.1. In Table 2.2, the various types of gas-liquid contactors commonly utilized in the chemical industries are presented. Explanations for each type of gas-liquid contactor are based on its hydrodynamic characteristics and mass transfer behavior. For flue gas desulfurization systems, various different types of gas-liquid contactors are being used. Presently, a number of pilot plants are either being planned or under construction. Summaries of their operations are provided by Devitt and Zada^[26], 1974; and Ando^[1], 1974. Other references relating to the application of gas-liquid contactors on the desulfurization processes are given in Table 2.3. It should be noted that Table 2.3 is provided according to the operational characteristics of these contactors.

2.2 Review of Turbulent Contacting Absorbers

The turbulent contacting absorber (TCA), first described in 1959^[55], is a scrubber primarily intended to remove particulates from a dust laden gas. TCA is a novel type of gas-liquid contacting device which consists of non-flooding packings made of low density

Table 2.1
 Classification of gas-liquid
 contactors. [2, 44, 45, 62]

Geometry of dispersed phase	Liquid drop, Gas bubble, Liquid film, Liquid jet.
Relative direction of flow of two phases	Cocurrent flow, Countercurrent flow, Crosscurrent flow
Type of operation	Batch system, Continuous system
Force utilized	Gravitational force, Centrifugal force

Table 2.2
Characteristics of gas-liquid contactors. [2, 7, 22, 37, 44, 45, 46, 53, 61, 62, 65, 68]

Type of Equipment	Flow Mechanism					Power Consumption		Mass Transfer
	Dispersed phase	Geometry of dispersed phase	Relative flow direction	Liquid surface renewal	Flow ratio	Phase in which power is supplied	Power Consumption effect on efficiency	Phase in which resistance predominates
Wetted Wall tower	(liquid)	(film)	cocurrent or counter- current	slight	variable	gas	slight	gas or liquid phase con- trolling
Bubble tower	gas	bubble	cocurrent or counter- current	slight	variable	gas	slight	liquid phase controlling
Agitated vessel with sparger	gas	bubble		slight	variable	gas	slight	
Packed tower	gas or liquid	film	cocurrent or counter- current	can be obtained with specific packings	variable	gas	slight	gas or liquid phase con- trolling
Wooden grid packed tower	liquid	film or drop	counter- current or cross- current	excel- lent	variable can be quite low	gas	slight	liquid phase controlling

Table 2.2 (Continued)

Type of Equipment	Flow Mechanism					Power Consumption		Mass Transfer
	Dispersed phase	Geometry of dispersed phase	Relative flow direction	Liquid surface renewal	Flow ratio	Phase in which power is supplied	Power Consumption effect on efficiency	Phase in which resistance predominates
Bubble cap tower	gas	bubble	counter-current (cross-current on a tray)	excellent	variable can be quite low	gas	slight	liquid phase controlling
Perforated plate tower	gas	bubble	counter-current (cross-current on a tray)	excellent	variable can be quite low	gas	slight	liquid phase controlling
Perforated plate tower without downcomer	gas	bubble	counter-current	excellent	variable can be quite low	gas	slight	liquid phase controlling
Rotational current tower	gas	bubble	counter-current (cocurrent on a tray)	excellent	variable can be quite low	gas	slight	liquid phase controlling

Table 2.2 (Continued)

Type of Equipment	Flow Mechanism					Power Consumption		Mass Transfer
	Dispersed phase	Geometry of Dispersed phase	Relative flow direction	Liquid surface renewal	Flow ratio	Phase in which power is supplied	Power Consumption effect on Efficiency	Phase in which resistance predominates
Spray tower	liquid	drop	counter- current or cocurrent	excel- lent	variable	liquid	significant	gas or liquid phase controlling
Centrifugal spray scrubber	liquid	drop	counter- current or cross- current	good	high	gas	significant	gas or liquid phase controlling
Cyclone scrubber	liquid	drop	cocurrent	slight	high	liquid	significant	gas phase controlling
Venturi scrubber	liquid	drop or bubble	cocurrent	slight	high	gas or liquid	significant	gas or liquid phase controlling
Jet scrubber	liquid	drop	cocurrent	good	high	liquid	significant	gas or liquid phase controlling
Centrifugal contactor	liquid	drop film and jet	counter- current or cocurrent	excel- lent	variable	gas (or equip- ment itself)	significant	gas or liquid phase controlling

Table 2.2 (Continued)

Type of Equipment	Flow Mechanism					Power Consumption		Mass Transfer
	Dispersed Phase	Geometry of dispersed Phase	Relative flow direction	Liquid surface renewal	Flow ratio	Phase in which power is supplied	Power Consumption effect on efficiency	Phase in which resistance predominates
Turbulent contacting absorber	liquid (gas)	film drop (bubble)	counter- current	excel- lent	variable	liquid	significant	gas phase controlling
Hydro- Filter scrubber	gas (in turbu- lent layer) liquid (other portion)	bubble drop	counter- current and cocurrent	fair	variable	liquid	significant	gas or liquid phase controlling

Table 2.3

Data on sulfur dioxide reduction using gas-liquid contactors.

Type of contactor	Removal process	SO ₂ vol %		Gas flow (kg/m ² hr)	Liquid flow (kg/m ² hr)	Liquid Gas ratio	Pressure loss (mm aq)	Absorption %	N _{OG}	K _{OG} ^a (kgmole/m ³ hr atm)	Reference	Remarks
		Inlet	Outlet									
Packed tower	Ammoniacal liquor process	0.3	0.06	2,100	4,000	1.6	<25	80	3.3	95	[2]	2" Raschig ring 20 moles NH ₃ / 100 moles H ₂ O
					6,700	2.7				250		
Wooden grid packed tower	Ammoniacal liquor process	0.15	0.018	4,750	2,800	0.5	<25	75	1.6	100	[2]	
			0.038	10,000	5,500			80	2.3	350		
Wooden grid packed tower	Ammoniacal liquor process	0.077	0.017	4,200	55,800	11.6		78	3.4	680	[2]	15.5 moles NH ₃ / 100 moles H ₂ O
Wooden grid packed tower	Lime process	0.128	0.01	5,000	4,800	0.5	<25	70	30		[2]	CaCO ₃ 10% slurries
		0.144	0.04	10,500	13,600	1.5		92	110			
Wooden grid packed tower	Lime process	0.08	0.006	11,000	32,000	3.2	76	93	2.4	24	[2]	
Wooden grid packed tower	Soda process	0.1	0.05	4,400		0.24	<25	50	0.75	143	[45]	0.5N NaOH solu.
		0.2	0.1	13,500	3,000	0.74			0.95	325		

Table 2.3 (Continued)

Type of contactor	Removal process	SO ₂ vol %		Gas flow (kg/m ² hr)	Liquid flow (kg/m ² hr)	Liquid gas ratio	Pressure loss (mm aq)	Absorption %	N _{OG}	K _{OG} ^a (kgmole/m ³ hr atm)	Reference	Remarks
		Inlet	Outlet									
Perforated plate tower	Ammoniacal liquor process	0.3	0.05	7,900	2,500	0.26	200	84	1.3	220	[2]	6 stages
				,	,	,	,	,	,	,		
Spray tower	Ammoniacal liquor process			9,400	3,200	0.37	260		2.7	260	[46]	
				,	,	,	,	,	,	,		
Spray tower	Lime process	0.3	0.03	1,300	1,700	1.3				15	[53]	Ca(OH) ₂ 6% slurries
				,	,	,				35		
Cyclone scrubber	Soda process	0.08	0.01	1,460	7,600	5.5		90	2.3	11	[44]	0.6N Na ₂ SO ₃ solu.
				,	,	,		,	,	,		
Venturi scrubber	Ammoniacal liquor process	0.17	0.03	3,000		0.26	<50	47	0.64	240	[2]	
				,	,	,		,	,	,		
Venturi scrubber	Ammoniacal liquor process	0.1	0.01	10,000		1.52		94	3.4	750	[68]	
				,	,	,		,	,	,		
Venturi scrubber	Ammoniacal liquor process	0.17	0.02	40		0.4	145	82	1.8	1,400	[2]	
				70 $\frac{m}{sec}$			380	94	3.5	4,300		
Venturi scrubber	Lime process	1.4	0.13	40		0.9	300	75	1.9	550	[2]	CaCO ₃ 10% slurries
				,		,	,	,	,	,		
Venturi scrubber	Lime process	1.6	0.3	50 $\frac{m}{sec}$		2.2	500	92	2.6	700	[2]	
				,		,		,	,	,		
Venturi scrubber	Lime process	0.13	0.02	60 $\frac{m}{sec}$		0.4	330	36	0.5	500	[2]	
				,		,	,	,	,	,		
Venturi scrubber	Lime process	0.14	0.08			2.1	620	86	2.0	2,200	[2]	

Table 2.3 (Continued)

Type of contactor	Removal process	SO ₂ vol %		Gas flow (kg/m ² hr)	Liquid flow (kg/m ² hr)	Liquid gas ratio	Pressure loss (mm aq)	Absorption %	N _{OG}	K _{OG} ^a (kgmole/m ³ hr atm)	Reference	Remarks
		Inlet	Outlet									
Venturi scrubber	Soda process	1.5	0.15	40	50 $\frac{m}{sec}$	0.26	300	90	2.3	520	[68]	Na ₂ CO ₃ solu.
				'		0.74	500			650		
Rotational current tower	Ammonia-water Oxygen-water					0.2			0.39	621	[61]	
						27.8			1.79	1,732		
Packed tower	Lime-stone slurry	0.2	0.04	1,995.8	7,308	2.8	2.54	45	0.6	55	[6]	1/2" intalox packing
		'	'	'	'	'	'	'	'	'		
TCA scrubber	Na ₂ CO ₃ solution	0.23	0.16	2,620.8	11,232	5.6	50.8	97	3.5	425	[29]	3 stages 5" packing/ stage
		0.09	0.001	7,459	48,060	3.2	53.34	90	2.3	104		
Hydro-filter scrubber	Na ₂ CO ₃ solution	0.12	0.012	14,918	101,196	13.6	317.5	99	4.6	417	[38]	
		0.12	0.0012	4,787	Bottom	Bottom	114	81	1.7	301	[29]	3/4" glass packing
			'	'	0~33,969	0~7.09	'	'	'	'	'	
			0.023	7,196	Top	Top	312	99	4.6	1,228	[38]	
Venturi and after scrubber	Na ₂ CO ₃ Solution	0.06	0.005	1,794*	7,962*	1.60	61	66	1.1	16	[29]	*only consider that in after scrubber
		'	'	'	'	'	'	'	'	'	'	
		0.12	0.041	4,971	24,840	13.8	330	92	2.5	101	[38]	

Table 2.3 (Continued)

Type of contactor	Removal process	SO ₂ vol %		Gas flow (kg/m ² hr)	Liquid flow (kg/m ² hr)	Liquid Gas ratio	Pressure loss (mm aq)	Absorption %	N _{OG}	K _{OG} ^a (kgmole/ m ³ hr atm)	Reference	Remarks
		Inlet	Outlet									
TCA scrubber	Lime-stone/ Lime-stone -MgO slurries	0.19	0.019	5,816	49,428	3.6	45.7	70	1.2	42	[10]	2~3 stages 10" packing/ stage
		0.31	0.093	13,658	119,520	20.55	254	99	4.6	382	[22]	
TCA scrubber	Lime slurry	0.24	0.017	13,709	113,400	8.27	152	60	0.9	75	[10]	2~3 stages 10" packing/ stage
		0.28	0.112		136,800	9.98	381	93	2.7	225	[22]	
Hydro-filter scrubber	Lime-stone/ Lime-stone MgO slurries	0.18	0.032	3,812	Bottom 0~34,248	Bottom 0~8.98	167	20	0.2	28	[29]	3/4" glass packing
		0.36	0.288	9,149	Top 0~11,509	Top 0~3.02	381	82	1.7	577	[38]	
Venturi and after scrubber	Lime-stone/ Lime-stone -MgO slurries	0.22	0.026	2,509*	0*	0	15.2	24	0.3	6.1	[29]	*only consider that in after scrubber
		0.34	0.26	6,490	23,888	9.52	330	88	2.2	115	[38]	
Venturi and after scrubber	Lime slurry	0.15	0.009	5,408*	47,776*	8.83	84	73	1.3	57	[29]	*only consider that in after scrubber
		0.35	0.095				96.5	94	2.8	122	[38]	

Table 2.3 (Continued)

Type of contactor	Removal process	SO ₂ vol %		Gas flow (kg/m ² hr)	Liquid flow ₂ (kg/m ² hr)	Liquid gas ratio	Pressure loss (mm aq)	Absorption %	N _{OG}	K _{OG} ^a (kgmole/ m ³ hr atm)	Reference	Remarks
		Inlet	Outlet									
Weir scrubber	Lime slurry	0.02	0.002	30,000	2,400	0.08	25.4	90	2.3		[66]	Horizontal Module 4 stages
		0.3	0.03	SCFM	gpm	gal/SCF						
Counter-current tray absorber	Lime-stone slurry	0.079	0.0011	5,581	36,534	2.3	25.4	58	0.9	59	[60]	2-3 stages
		0.242	0.1	15,859	109,589	19.64	254	99	4.8	891		

spheres placed between retaining grids. Due to the counter-current gas and liquid flows, the spheres are forced upward in a random, turbulent motion, promoting intimate mixing between gas and liquid. The effect of the turbulent action is two fold. First, gas and liquid are brought together for a thorough interfacial contact. Second, the moving spheres are continuously cleaned by the tumbling action which effectively prevents solids build-up and thus eliminating channeling, plugging and fouling. The use of TCA permits much greater gas and liquid velocities than are possible in conventional scrubbers. Thus, a smaller tower may be employed for a given operation.

In recent years a number of studies relating to hydrodynamic, mass and heat transfer in TCA have become available. (Kulbach^[49], 1961; Douglas et al.^[27], 1963; Douglas^[28], 1964; Gel'perin et al.^[39], 1965; ^[40], 1966; Blyakher et al.^[8], 1967; Levsh et al.^[50], 1967, ^[51], 1968; Gel'perin et al.^[41], 1968; Chen and Douglas^[23], 1968, ^[24], 1969; Balabekov et al.^[3], 1969; Khanna^[47], 1971; Barile and Meyer^[5], 1971; Borgwardt^[10], 1972; O'Neill et al.^[57], 1972; Tichy et al.^[63], 1972; Tichy and Douglas^[64], 1973; Epstein^[29], 1973; Barile et al.^[4], 1974; McMichael et al.^[52], 1975; Kito et al.^[48], 1975). However, the information on operational characteristics are still fragmentary and the data reported are, in many instances, contradictory.

In studying hydrodynamic phenomena of TCA, Gel'perin et al.^[40], (1966) reported that liquid hold-ups, bed expansions, flow behavior

and pressure drop are significantly affected by the liquid and gas flow rates. Contrary to the usual practice of TCA grid arrangement which provides large free area to allow large flow rate, in their study, the free area of grids are rather small. Consequently the pressure drop data which include large pressure drop across the grids are not of practical interest. Levsh et al.^[50], (1967) presented a correlation for the low density disk packing and found that pressure drop increases linearly with the gas flow rate. Blyakher^[8], (1967) studied the pressure drop and separated the effect of total pressure drop into components of contributions. They are contributions due to the dry grid, the dry packing of the bed, the liquid hold-up on the grid and the liquid hold-up of the packing. Similar analysis for pressure drop was later presented by Gel'perin et al.^[41], (1968).

Liquid hold-up, bed expansion and minimum fluidization velocity in TCA were measured and correlated by Chen and Douglas^[23], (1968). The liquid hold-up was found to be independent of gas flow rate. However, the effect of both liquid flow rate and packing diameter appear to be similar to that reported for the conventional fixed bed absorbers. The minimum fluidization velocity was observed to vary with packing diameter and liquid flow rate. In addition to these variables the bed expansion correlation is also a function of gas flow rate. Chen and Douglas^[24], (1969) studied the liquid mixing behavior for TCA. Liquid mixing data in terms of Peclet number was correlated as a function of the Peclet number in fixed bed, the ratio

of packing diameter to column diameter and $(u - u_{mf})/u_{mf}$. Experimental study for similar hydrodynamic parameters was also carried out by Khanna^[47](1971). In his investigation, wider liquid and gas flow rates than that reported by Chen and Douglas^[23, 24], (1968, 1969) were examined. In addition, the gas-liquid interfacial area composed of liquid drops, liquid film and gas bubble was considered and correlated in terms of hydrodynamic properties.

C'neill et al.^[57], (1972) classified the mode of gas-liquid contacting operation in a tower containing fluidizing packings into two types: type 1, fluidization in the absence of incipient flooding and type 2, fluidization due to incipient flooding. TCA scrubber utilizes very low density packings, hence, is classified as type 1. In this mode of operation, the gas flow rate is increased at a constant liquid flow rate until the upward force of liquid flow balances the weight of packing plus the liquid hold up which is equal to the total pressure drop. The gas velocity at this point is identifying below the flooding velocity.

Static pressure within the expanded bed in TCA was measured by Tichy et al.^[63], (1972). They reported that the static pressure was linearly proportional to the height of the bed. Using the pressure drop as the criterion, Tichy and Douglas^[64], (1973) later classified the TCA into three hydrodynamic regimes. These are static bed, semi-mobile bed and fully mobile bed. In fully mobile bed, it is divided into three regions, i.e., constant liquid hold-up region, increasing liquid hold-up region and flooding region.

For the mass and heat transfer studies in TCA, Douglas et al.^[27], (1965) investigated the absorption of CO_2 and SO_2 from dust-laden gas by alkaline solution. The condensation of steam from the gas mixture containing steam, air and H_2S emitted from pulp digesters was observed to significantly increase the mass transfer coefficient over that in packed tower. Subsequently, the gas absorption data of NH_3 by boric acid solution was reported by Douglas^[28], (1964). The experimentation was conducted for a dehumidification and cooling of hot air saturated with steam. It was found that the height of overall mass transfer unit for the NH_3 absorption was approximately 1/2 to 1/3 of that obtained in a packed bed. Furthermore, significant increase in mass transfer was observed for the dehumidification and cooling system. TCA used as a cooling tower for heated power-plant cooling water was developed and analyzed by Barile and Meyer^[55], (1971) and Barile et al.^[4], (1974). They revealed that a 20°F cooling range can be easily achieved in a one foot packing bed.

The absorption of SO_2 by alkaline solutions and slurries in TCA has recently been studied in a small scale scrubber (Borgwardt^[10-22]) and a large scale scrubber (Epstein^[29-38]). A significant improvement in SO_2 removal efficiency was observed for TCA compared with that using conventional packed tower and venturi scrubber. The extensive data reported from these units were analyzed. Meanwhile, a mathematical model was presented to describe the SO_2 absorption process using limestone/lime slurries. (McMichael et al.^[52], 1975).

Kito et al.^[48], (1975) measured the gas-liquid interfacial area

and gas side mass transfer coefficient is a TCA with stagnant liquid. However, the liquid side mass transfer coefficient for TCA has so far not been investigated.

2.3 Review of the Chemistry of SO₂ Scrubbing Using Limestone/Lime Slurries

2.3.1 Chemical Reaction in SO₂ Absorption

Perhaps, the most difficult problem in SO₂ scrubbing by limestone/lime slurries is associated with the understanding of the chemical reactions in the liquid phase. In addition to the presence of a number of solid constituents numerous ionic and neutral species are also present in the liquid phase. Examples of the major components present are HSO₃⁻, SO₃⁼, CaSO₃, HSO₄⁻, MgSO₃, HSO₄⁻, H₂SO₃, SO₄⁼, Ca⁺⁺, CaHCO₃⁺, HCO₃⁻, MgHCO₃⁺, CO₃⁼, H₂CO₃, CaOH⁺, OH⁻, H⁺, Mg⁺⁺, CaCO₃, etc. An attempt is made here to determine the key ionic or neutral reactions associated with the SO₂ absorption in the overall scrubbing analysis. Several reaction mechanisms have been proposed. However, considerable additional information is needed to determine the key mechanism. Boll^[9], (1970) found from his mathematical model study that the chemical reaction was approximately of the first order with respect to both the partial pressure of SO₂ in equilibrium with the bulk liquid and the surface area of the limestone. In view of the complicated equilibrium phenomena involving multiple phases and chemical reactions, Potts et al.^[58], (1971) presented schematically the interrelationship between gas, liquid and solid for the system

containing CaO , SO_2 , SO_3 , CO_2 and H_2O . The complex processes of chemical and diffusional steps, including gas diffusion and solid dissolution, were explained by Slack et al.^[59], (1972). Experimental performance of SO_2 absorption in limestone slurry in a laminar jet absorber was studied by Bjerle et al.^[7], (1972). It was shown that the controlling reaction mechanism in the pH range between 8 to 9 was the irreversible and instantaneous reaction between total SO_2 and HCO_3^- . In addition, it was observed that the SO_2 absorption rates were practically equal for different scrubbing solutions including 0.1 M HCO_3^- with pH of 8.3 and 0.1 M NaOH. However, Vivian^[65], (1973) conducted an experiment in a short wet wall column revealing that the chemical reaction was governed by the irreversible and instantaneous reaction between SO_2 and the hydroxyl ion forming bisulfite and sulfite ions. The liquid employed in his experiment was lime slurry with pH ranging from 12 to 13. Deducing from the mathematical model analysis, McMichael et al.^[52], (1975) recently concluded that the absorbed SO_2 in form of H_2SO_3 reacts instantaneously and irreversibly with OH^- , HCO_3^- , CaHCO_3^+ and MgHCO_3^+ ions as it diffuses into the liquid phase. This view was shown to be, in part, consistent with previous investigators (Bjerle, et al.^[7], (1972); Vivian^[65], (1973)) and can partially explain the SO_2 scrubbing data using limestone slurries. However, more studies are necessary to clarify this conclusion.

2.3.2 Oxidation and Solid Precipitation in the Slurries

One of the most important factors in optimizing the performance of SO_2 scrubbing systems using limestone/lime slurries is control of the slurry pH (Borgwardt^[10-22], Epstein^[29-38]). Differences in pH affect the operation of a limestone/lime scrubber in two ways (Cheremisinoff and Fellman^[25], (1974)): (1) Operating at a low pH decreases the solubility of CaSO_4 , therefore, promotes the formation of calcium sulfate dihydrate, gypsum, precipitation. (2) Operating at a high pH decreases the solubility of CaSO_3 , therefore, promotes the formation of calcium sulfite precipitation. Apparently, there exists an optimum pH at which the precipitation of both sulfate and sulfite becomes minimum. However, it should be noted that the solid precipitation produced by calcium sulfite are soft and delicate and easily altered mechanically, while the precipitation formed by gypsum is characterized by hard and stubborn scale. The scale seriously hinders the continuous operation of the tower by plugging the surface of the grid. The source of gypsum is the oxidation of calcium sulfite by dissolved oxygen. This reaction occurs in an aqueous solution and is favored at low pH (Borgwardt^[22], (1974)).

Only recently it was realized that subsaturation of calcium sulfate dihydrate in the scrubbing liquid could be achieved in a closed system. Although this finding was first reported by ICI (Imperial Chemical Industries) in 1935. The results of ICI's experience were recently confirmed in pilot tests conducted by Borgwardt^[22], (1974). Operation with the scrubbing liquid unsaturated with respect to dissolved calcium sulfate dihydrate presents an opportunity to reduce

gypsum scaling. The subsaturation mode is achieved by the precipitation of calcium sulfate occluded by the precipitant of calcium sulfite. A solid solution formed by this mode is being identified. (Borgwardt^[22], (1974)). It is also found that the quantity of calcium sulfate that can be occluded is directly related to the sulfate activity in the scrubbing liquid and the sulfite precipitation rate. Experimental data also show that Cl^- ion has the effect of suppressing the sulfate activity while Mg^{++} ion could raise its activity. Fly ash was found to have no significant effect on the operations of SO_2 scrubbing using limestone/lime slurries.

Chapter 3

Mathematical Model for SO₂ Absorption in Spray and TCA Scrubbers

3.1 Introduction

Among the wet processes using limestone slurries in scrubbing SO₂ from flue gases, two of the most promising scrubbers for carrying out the limestone scrubbing appear to be the turbulent contacting absorber (TCA) and the spray column. Several large scale scrubber-holding tank recycle systems have been built and sponsored by the EPA to test the performance and reliability of these scrubbers.

In this chapter experimental data from the large scale TCA scrubber and spray column located at the TVA Shawnee power station and the EPA TCA scrubber at Research Triangle Park, North Carolina, are analyzed to obtain equations and correlations which can be used to design and scale-up spray column and TCA scrubbers which utilize limestone slurries to scrub SO₂ from flue gases.

In subsequent sections a mathematical model is developed which describes the absorption of SO₂ by limestone slurries in a scrubber; parameters appearing in this model are evaluated from experimental data and correlated in terms of the operating parameters; and the experimentally observed SO₂ removal efficiency is compared to the efficiency computed from the model.

3.2 Mathematical Models of Spray and TCA Scrubbers

In the analysis and design of contacting devices used for the

scrubbing of SO_2 from flue gas with limestone slurries the mass transfer coefficients which describe the SO_2 fluxes in the gas and liquid phases should be known. The gas film mass transfer coefficients for physical absorption are relatively easily obtained from experimental data; on the other hand, the liquid film coefficient for physical absorption is difficult to determine due to chemical reactions (such as dissociation) which will occur upon the absorption of a gas molecule into a liquid phase. In the present case, where the mechanism of the absorption of SO_2 into limestone slurry is not well understood, it does not appear possible, at the present time, to determine the liquid side mass transfer coefficient for physical absorption for large scale scrubbers from experimental data on scrubbing SO_2 from flue gases with limestone slurries.

In this section a mathematical model for the spray column and TCA scrubbers is developed. Gas side mass transfer coefficients which have been previously reported in the literature or obtained from experimental data in this study are presented for each column. The liquid film resistance to the transfer of SO_2 into limestone slurries, determined from experimental data, is correlated in terms of the ratio of the gas and liquid film resistances. This ratio of the resistances appears to be only a function of the magnesium concentration, pH of the slurry, SO_2 partial pressure in the gas phase and type of scrubber within the accuracy of the experimental data.

3.2.1 Scrubber Model

Scale drawings of the scrubbers to be considered in this study are given in Figures 3.1, 3.2 and 3.3. In the TVA Shawnee TCA scrubber, as shown in Figure 3.1, the scrubbing slurry is sprayed from a single arrangement of nozzles at the top of the column and falls through a series of grids and areas filled with "ping pong" balls. Actually the TCA has also been operated without the spherical packing pieces and in this situation the column is referred to as the "TCA without packing spheres". Flue gas containing SO_2 in concentrations up to 4500 ppm passes counter-currently to the limestone slurry. The spray column with four spray headers shown in Figure 3.2 is slightly more complicated than the TCA without spheres in that the scrubbing slurry is sprayed at four levels. However, as will be shown later, this situation is easily handled and the column can be described mathematically in terms of the mass transfer coefficients for the TCA without packing spheres. In Figure 3.3 a scale drawing of the EPA/RTP TCA scrubber is given.

The TVA Shawnee TCA and spray column treat flue gas at a rate equivalent to a 50 MW power station and have cross-sections which are square (5 ft. edge) and circular (8 ft. dia.), respectively. The EPA/RTP is approximately 9 inches in diameter.

For the TCA operating with packing spheres, the column is divided into packed and unpacked sections; and mass transfer coefficients are used to describe the respective sections.

The molar flux of SO_2 across the gas-liquid interface of a packed or unpacked section of a wet scrubber can be written in terms of the

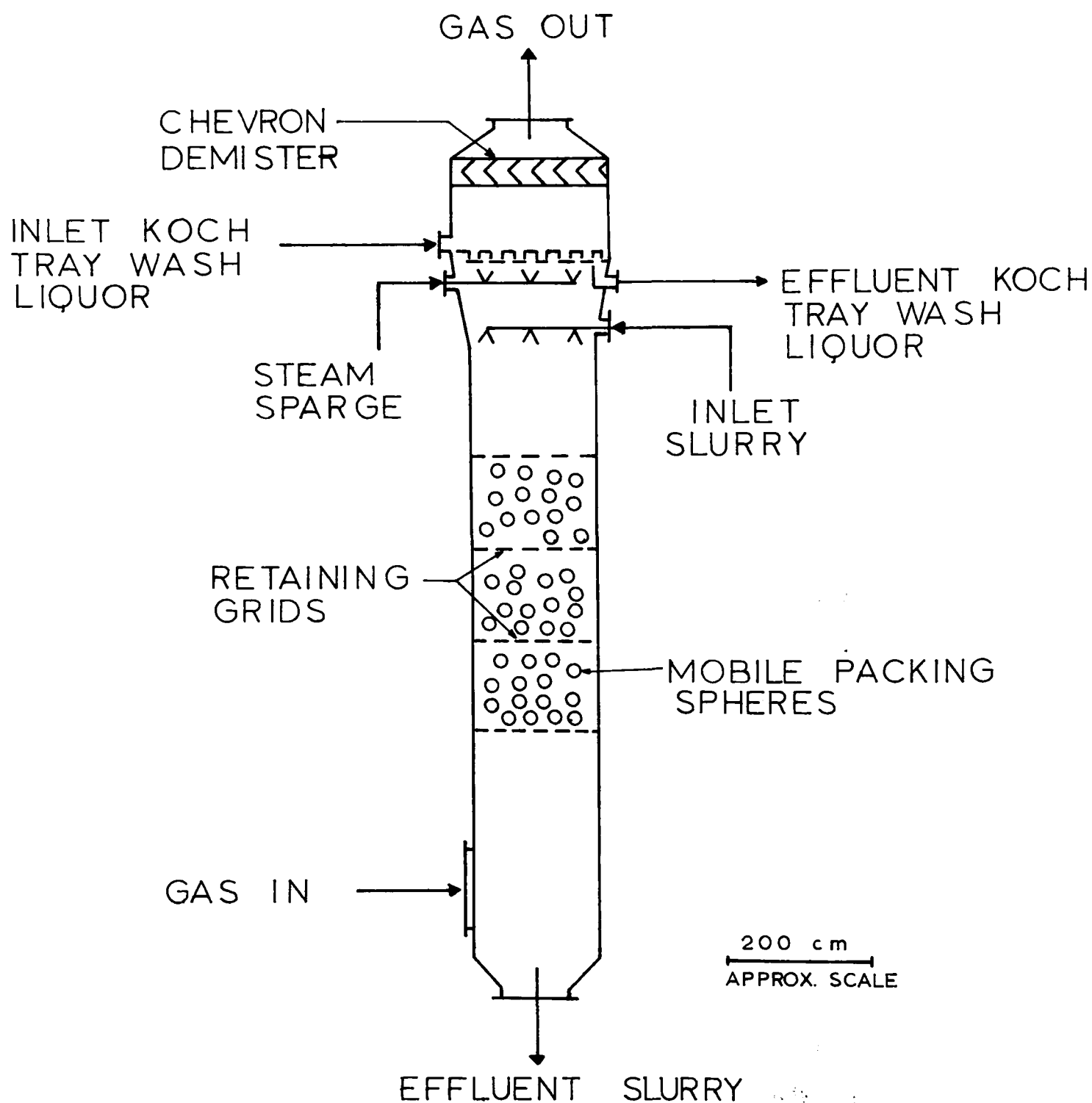


Figure 3.1 Schematic of TVA Shawnee Three-Bed TCA (Epstein^[37]).

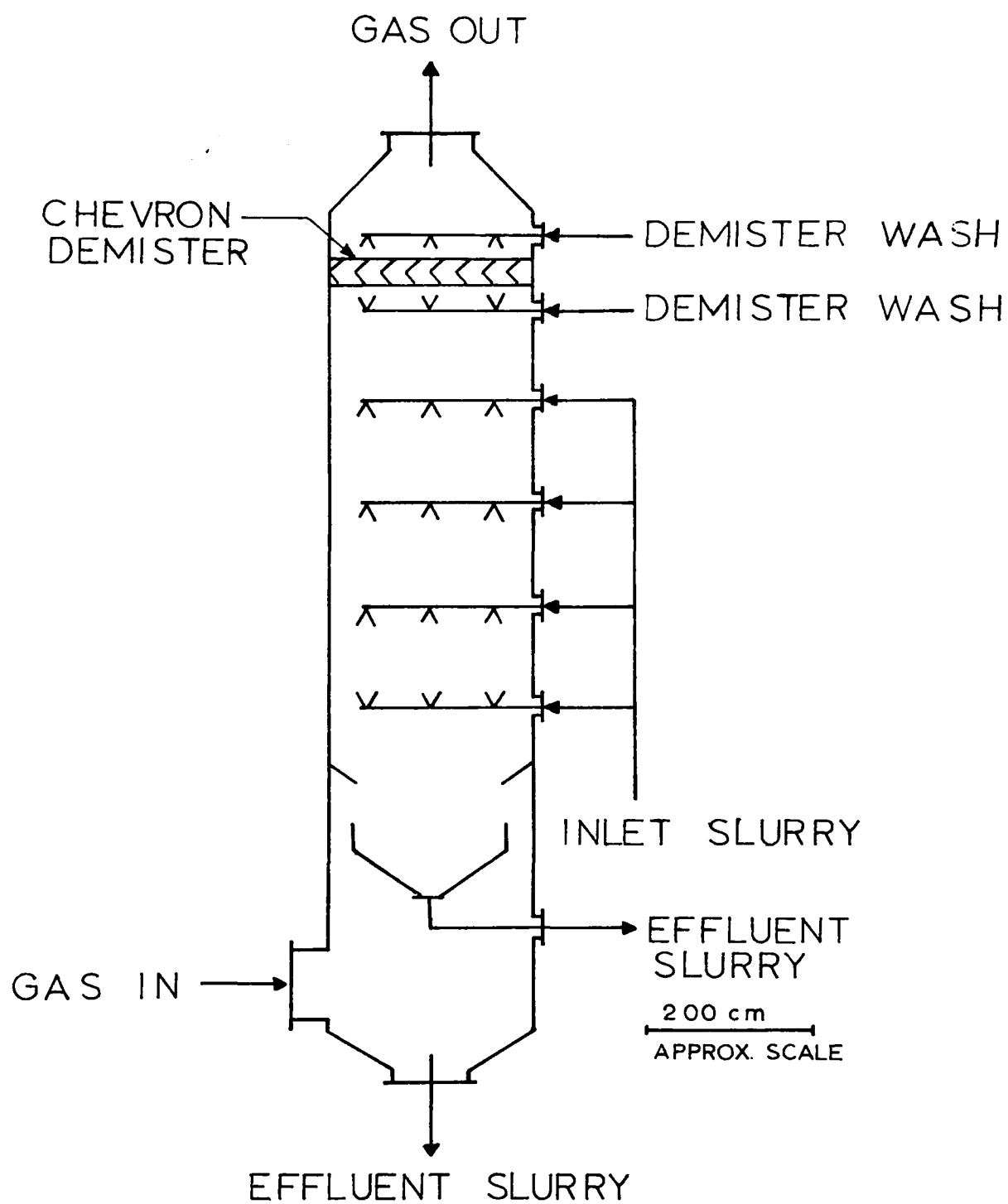


Figure 3.2 Schematic of TVA Shawnee Spray Tower (Epstein^[37]).

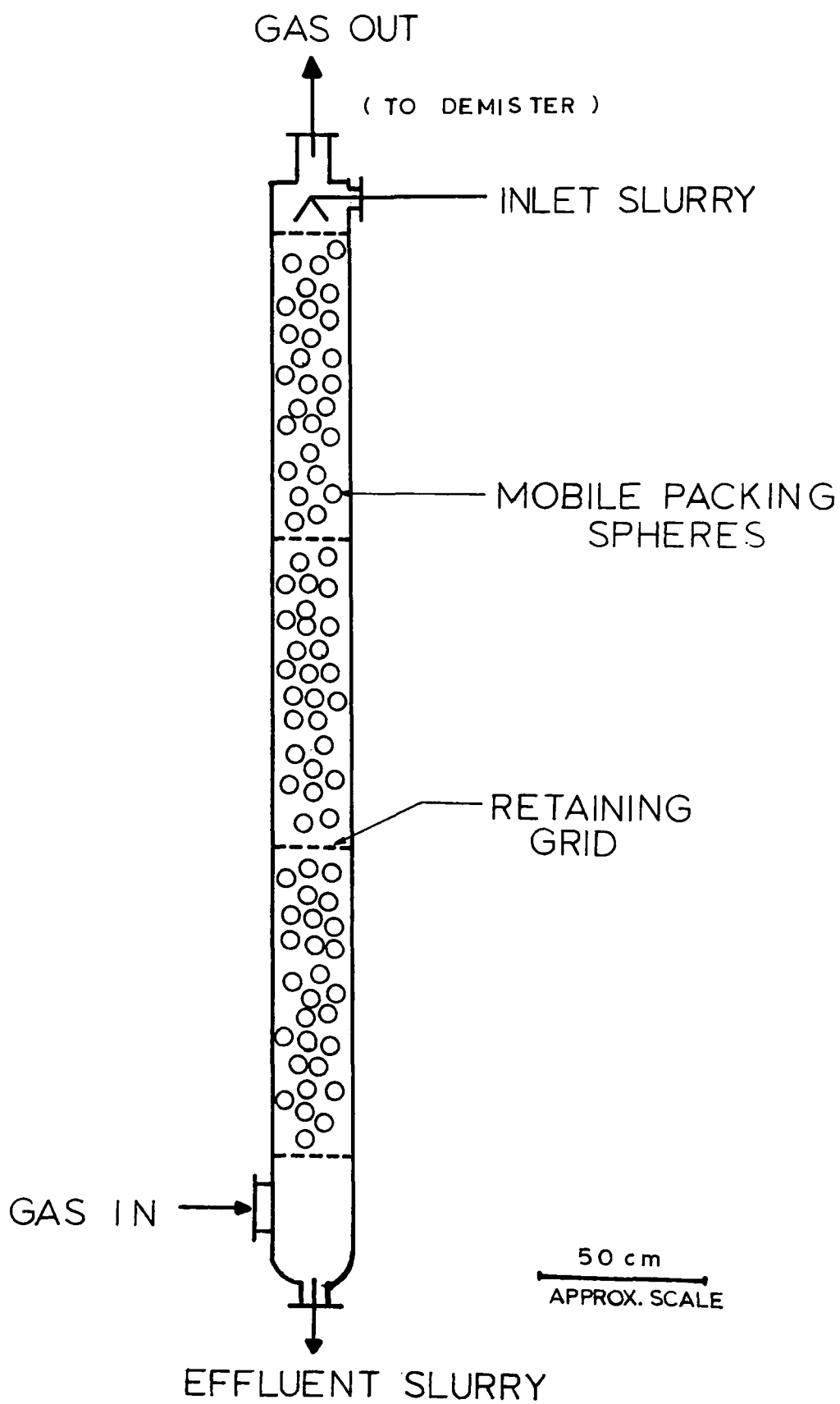


Figure 3.3 Schematic of the EPA/RTP Research TCA Scrubber (Borgwardt^[10]).

gas or liquid side resistance as

$$N_{SO_2} = k_g (P_{SO_2} - P_{SO_2}^i) = k_L^\circ \phi (C_{Ai} - C_A) \quad (3-1)$$

where k_L° is the liquid film mass transfer coefficient for physical absorption, (cm/sec),

k_g is the gas side mass transfer coefficient for physical absorption, (gmol/cm² atm sec),

N_{SO_2} is moles of SO₂ absorbed per unit time per unit interfacial area, (gmol/cm² sec),

ϕ is the enhancement for mass transfer in the liquid film due to chemical reaction, (dimensionless),

P_{SO_2} is the partial pressure of SO₂ in the bulk gas phase, (atm),

$P_{SO_2}^i$ is the interfacial pressure of the SO₂, (atm),

C_{Ai} is the H₂SO₃ concentration at the gas-liquid interface, (gmol/cm³),

and C_A is the H₂SO₃ concentration in the bulk liquid phase, (gmol/cm³).

The enhancement factor, ϕ , takes into account the reaction of the diffusing H₂SO₃ with components found in the liquid phase.

The concentration of H₂SO₃ at the gas-liquid interface, C_{Ai} , can be related to the partial pressure of SO₂ at the interface, $P_{SO_2}^i$, by Henry's law

$$P_{SO_2}^i = H C_{Ai} \quad (3-2)$$

where H is the Henry's law constant, (atm cm³/gmol).

This equation holds for sufficiently dilute solutions.

The Henry's law constant, H , as a function of temperature has been given by Vivian^[65], (1973) as

$$\ln H = 17.360 - \frac{3175.2}{T} \quad (3-3)$$

where T is the liquid temperature in degrees Kelvin.

An expression for the interfacial concentration of H_2SO_3 , C_{Ai} , can be obtained by substituting Equation (3-2) into (3-1).

$$P_{SO_2}^i = \frac{k_g P_{SO_2} + \frac{k_L^\circ}{H} \phi P_{SO_2}^*}{k_g + \frac{k_L^\circ}{H} \phi} \quad (3-4)$$

where $P_{SO_2}^*$ is the partial pressure of SO_2 which could be maintained in equilibrium with the bulk liquid phase, (atm).

Substitution of this equation into Equation (3-1) gives

$$N_{SO_2} = \left(\frac{1}{k_g} + \frac{H}{k_L^\circ \phi} \right)^{-1} (P_{SO_2} - P_{SO_2}^*) \quad (3-5)$$

The rate of SO_2 absorption in a differential height of the scrubber, dz , can be written as

$$\frac{-G}{P_T} \frac{dP_{SO_2}}{dz} = \left(\frac{1}{k_g a} + \frac{H}{\phi k_L^\circ a} \right)^{-1} (P_{SO_2} - P_{SO_2}^*) \quad (3-6)$$

In Equation (3-6) both ϕ and $P_{SO_2}^*$ are functions of position in the column and both depend on the mechanism of SO_2 absorption into recycled limestone slurries. For a calcium carbonate, calcium sulfite, carbon dioxide, sulfur dioxide and water system at equilibrium and a pH greater than 4.7, the equilibrium SO_2 partial pressure of the aqueous system will usually be much less than the SO_2 partial pressure

found in the flue gas (i.e., $P_{SO_2} \gg P_{SO_2}^*$ for $pH > 4.7$). Thus $P_{SO_2}^*$ can be ignored relative to P_{SO_2} in Equation (3-6) to give

$$\frac{-G}{P_T} \frac{dP_{SO_2}}{dz} = \left(\frac{1}{k_g a} + \frac{H}{\phi k_L^o a} \right)^{-1} P_{SO_2} \quad (3-7)$$

Equation (3-7) can be integrated over the height of the column section (from Z_1 to Z_2) to give

$$\frac{G}{P_T} \ln \frac{P_{SO_2}(Z_1)}{P_{SO_2}(Z_2)} = \int_{Z_1}^{Z_2} \left(\frac{1}{k_g a} + \frac{H}{\phi k_L^o a} \right)^{-1} dz = \int_{Z_1}^{Z_2} K_G a \, dz \quad (3-8)$$

where $K_G a = \left(\frac{1}{k_g a} + \frac{H}{\phi k_L^o a} \right)^{-1}$ is the overall gas side mass transfer coefficient, ($\text{gmol}/\text{cm}^3 \text{ atm sec}$).

Applying the mean value theorem to Equation (3-8) yields

$$\frac{G}{\Delta Z P_T} \ln \frac{P_{SO_2}(Z_1)}{P_{SO_2}(Z_2)} = \overline{K_G a} = \left(\frac{1}{k_g a} + \frac{H}{\overline{\phi} k_L^o a} \right)^{-1} \quad (3-9)$$

where $\overline{\phi}$ and $\overline{K_G a}$ are the "average" enhancement factor and the "average" overall mass transfer coefficient, respectively.

and $\Delta Z = Z_2 - Z_1$.

Large values of the enhancement factor, $\overline{\phi}$, correspond to the gas film being the dominating resistance to the transfer of SO_2 ; and small values of the enhancement factor indicate that the liquid film resistance is important. If the gas and liquid film mass transfer coefficients for physical absorption can be calculated, it is possible to separate the liquid film mass transfer coefficient, $k_L a$, into a chemical reaction term (i.e., the enhancement factor, $\overline{\phi}$), and

the liquid film mass transfer coefficient for physical absorption, $k_L^o a$.

However, for the Shawnee and EPA scrubbers being analyzed in this study, it does not appear possible to calculate the liquid film mass transfer coefficients for physical absorption from the data reported. Thus, the separation of the liquid film mass transfer coefficient into chemical reaction and mass transfer effects cannot be made at this time. It is obvious that such a separation is desirable since it may result in a simplification of the data and lead to a general mathematical model for various scrubbers.

The second equation of Equation (3-9) can be arranged to give

$$R = \frac{\overline{\phi k_L^o a}}{H \overline{k_g a}} = \frac{\overline{K_G a}}{\overline{k_g a - K_G a}} \quad (3-10)$$

The overall coefficient, $\overline{K_G a}$, can be calculated from experimental data using the first equation of Equation (3-9). The gas film mass transfer coefficient, $\overline{k_g a}$, can be calculated by methods to be discussed below.

The left hand side of Equation (3-10) (or the definition of R) can be interpreted as the ratio of the gas film resistance to mass transfer and the liquid film resistance. The larger this ratio the more the SO_2 transfer in the column is controlled by the gas film. As will be shown below the ratio of resistances appears to be an effective method of correlating liquid film resistances.

3.2.2 Mass Transfer Coefficients

The gas side mass transfer coefficient for physical absorption in

the Shawnee TCA operating without packing spheres has been reported by Epstein^[37] as

$$k_g^s a = 0.00134 G^{0.8} L^{0.4} \quad (3-11)$$

where a is the interfacial area available to mass transfer per unit volume of the column, (cm^2/cm^3),

G is the molar gas flow rate, ($\text{gmol}/\text{cm}^2 \text{sec}$),

and L is the mass flow rate of the liquid phase, ($\text{g}/\text{cm}^2 \text{sec}$).

This correlation is based on experiments on SO_2 absorption into sodium carbonate solutions which had pH's in the range from 6.75 to 9.5.

At these high pH's the transfer of SO_2 into these solutions can be assumed to be gas film controlled. (Epstein^[37], 1973)

The gas film mass transfer coefficient for the Shawnee TCA operating without packing spheres can also be applied to the Shawnee spray column. Epstein^[38] has reported data for a limestone depletion run in the Shawnee spray column in which the initial pH of the scrubbing slurry was 7.30. The Shawnee spray column with 4 spray headers can be divided into 4 sections. The top section of the column has a liquid flow rate of $1/4 L$, the next a liquid flow rate of $1/2 L$ and so on until in the bottom and fourth section the liquid flow rate is equal to L . Assuming the same liquid flow rate dependence (i.e., $L^{0.4}$) in the Shawnee spray column as in the Shawnee TCA without spheres, Equation (3-9) can be written as

$$\begin{aligned} \frac{G}{P_T} \ln \frac{P_{SO_2}^{in}}{P_{SO_2}^{out}} &= C_1 G^m L^{0.4} \left[\left(\frac{1}{4}\right)^{.4} Z_1 + \left(\frac{1}{2}\right)^{.4} Z_2 + \left(\frac{3}{4}\right)^{.4} Z_3 + Z_4 \right] \\ &= k_g a(G, L) \sum_{i=1}^4 \left(\frac{i}{4}\right)^{.4} Z_i \end{aligned} \quad (3-12)$$

where Z_i is the length of the i^{th} section and m and C_1 are constants. Using Epstein's limestone data at a pH of 7.30 and the above equation, the gas film coefficient for the Shawnee spray column is calculated to be $k_g a = 1.65 \times 10^{-5}$ gmole/cm³ atm sec at a gas flow rate of $G = 0.00548$ gmole/cm² sec and a total liquid rate of $L = 0.652$ g /cm² sec. The gas film coefficient calculated using Epstein's correlation (Equation 3-11)) would give $k_g^s a = 1.75 \times 10^{-5}$ gmole/cm³ atm sec at the same flow conditions. It can be seen that Epstein's correlation for the gas film coefficient in the Shawnee TCA operating without packing spheres can predict the gas film coefficient for the Shawnee spray very accurately; and in the absence of more data it is assumed that the gas film coefficient for both the Shawnee spray column and the TCA without packing spheres can be given by Epstein's correlation (Equation 3-11)).

The ratio of the mass transfer resistance of the gas film to that of the liquid film can be calculated for the Shawnee TCA without packing spheres and the Shawnee spray column with 4 spray headers from the data of Epstein^[37,38]. The values of R obtained for these scrubbers are shown in Figure 3.4 as a function of the inlet pH. The range of operating conditions for the data shown in Figure 3.4 are given in Table 3.1.

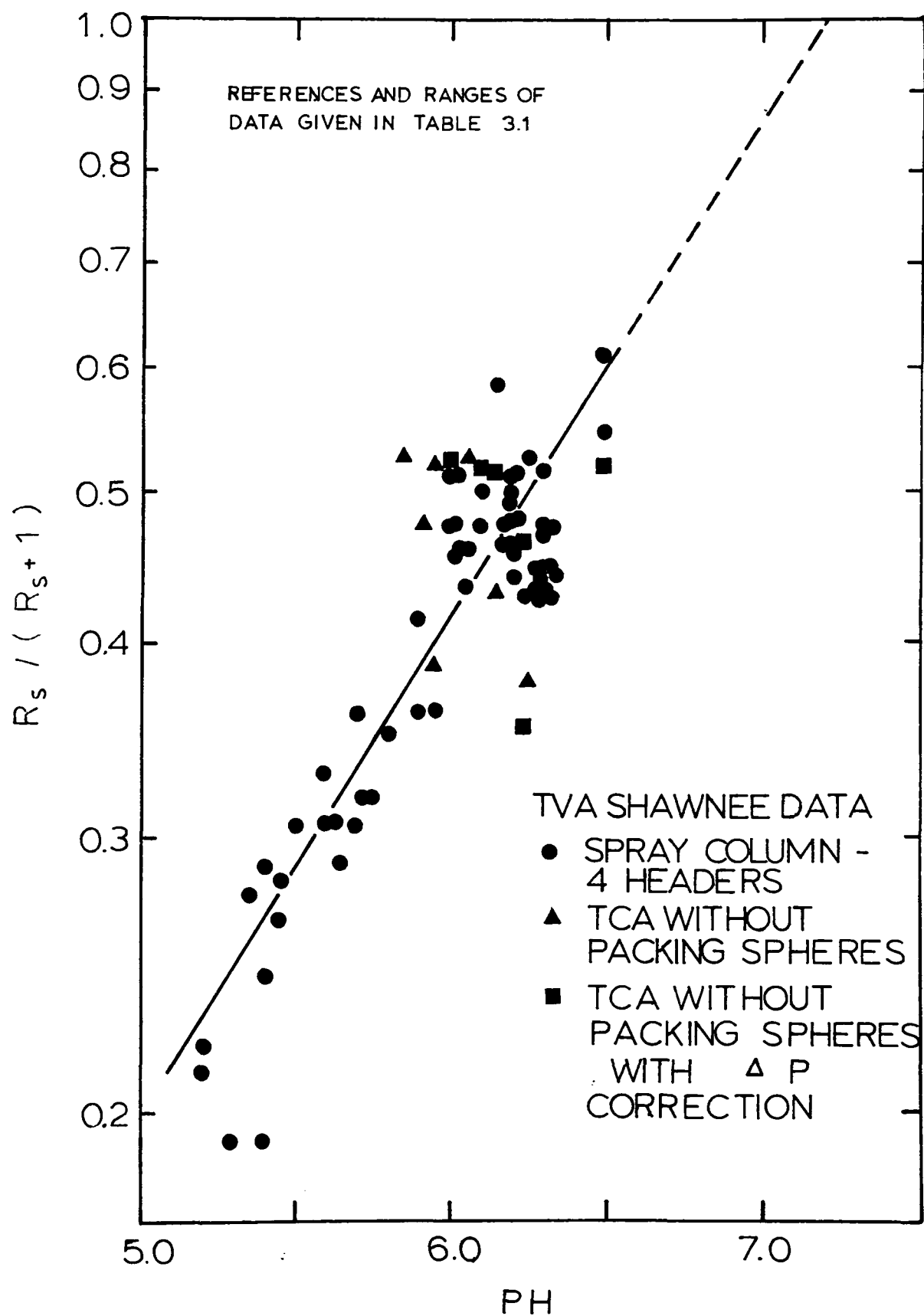


Figure 3.4 Ratio of the Mass Transfer Resistances for Spray Devices, R_s , as a function of the pH of the Scrubbing Slurry at the Inlet of the Scrubber.

Table 3.1

Range of Data for the Shawnee Spray Column and TCA Operating Without Packing
Spheres Used in Constructing Figure 3.4

Equipment and References	pH	G ($\frac{\text{gmole}}{\text{cm}^2 \text{ sec}}$)	L ($\frac{\text{g}}{\text{cm}^2 \text{ sec}}$)	Inlet Slurry Temperature (°F)	Inlet P _{SO₂} (ppm)	ΔP (in. H ₂ O)	Mg Concentration in slurry (ppm)
Spray Column	5.30				1750	not	less
4 spray headers ^[38]	to 7.30	0.00548	0.652	97 to 113	to 3187	reported	than 350
TCA without Packing spheres ^[37]	5.85 to 6.4	0.00687 to 0.01378	0.886 to 2.86	58 to 119	1850 tp 3300	1.0 to 5.8	less than 350

For some of the data used in Figure 3.4 very high pressure drops along the length of the column with respect to the pressure drop which would normally be expected at the same gas and liquid flow rates were observed. This high pressure drop was probably due to scaling and its effect on increasing the liquid hold-up in the scrubber. Also at these high pressure drops a higher than normal SO_2 absorption efficiency has observed. It was found that the high pressure drop data could be made to agree with the normal pressure drop data in Figure 3.4 if the gas film mass transfer coefficient was given by

$$k_g^s = 0.00134 G^{0.8} L^{0.4} \left(\frac{\Delta P}{\Delta P_N} \right)^{0.4} \quad (3-13)$$

where ΔP_N is the pressure drop without scaling of the column,

(in. H_2O),

and ΔP is the observed pressure drop, (in. H_2O).

This equation is exactly the same as Epstein's correlation (Equation (3-11)) for the gas film coefficient for the spray column except it includes the pressure drop correction.

The pressure drop without scaling, ΔP_N , can be correlated^[67] in terms of the gas and liquid flow rates as

$$\Delta P_N = 0.481 L^{0.6} G^{1.17} Z_T \quad (3-14)$$

where Z_T is the total height of the spray section, (cm).

The ratio of mass transfer resistances, R , was correlated in terms

of inlet slurry pH for several reasons:

- 1) The inlet slurry pH was readily available.
- 2) The amount of SO_2 absorbed per liter of slurry is relatively small and the slurry residence time fairly short and therefore, the average condition of the slurry in the scrubber could be reflected in its initial pH.
- 3) The inlet pH was used because this pH is more easily determined in a recycle system than the pH of the outlet slurry from the scrubber. In a recycle system with fairly large holding tank residence times the liquid phase will approach equilibrium and under this condition the composition of the liquid is fixed at a given pH, temperature and partial pressure of CO_2 above the holding tank. Many species in limestone slurries are insensitive to the CO_2 partial pressure and very sensitive to the pH.

The effect of SO_2 partial pressure on the scrubbing efficiency of limestone slurry has been recognized by Gleason^[42], (1971) and Nannen et al.^[54], (1974). These authors have noted that as the partial pressure of SO_2 in the flue gas decreases the SO_2 transfer becomes more gas film controlled. In accordance with this observation the ratio of the mass transfer resistance of the gas film to that of the liquid film should increase with a decrease in SO_2 partial pressure in the flue gas. For the spray type devices discussed above, the dependence of R on the SO_2 partial pressure could not be distinguished above the scatter of the data; nor could a dependence of R on the hydrodynamics be established for the spray devices.

The scatter in the data in Figure 3.4 could be due in part to the

fact that the raw data used to calculate the ratio of resistances, R , was reported in ranges and the average of the reported ranges was used to calculate the value of R .

In Figure 3.4 it can be seen that the extrapolation of the straight line through the data points to a value of $R_s/(R_s+1)$ equal to one given a pH of 7.2 as the pH above which the SO_2 absorption is gas film controlled. This is in agreement with the assumption that the SO_2 absorption was gas film controlled at a pH of 7.3 in the case of the limestone depletion run for the Shawnee spray column.

For the TCA operation with packing spheres the column must be divided into two sections: one corresponding to the section filled with packing spheres, and another where there are no packing spheres and the column behaves much like a spray device. This situation is illustrated in Figure 3.5. The reason for this separation is that the packed and spray sections will have significantly different contacting mechanisms and consequently different mass transfer coefficients. Also this separation is desirable so that columns with different packing heights can be compared.

An actual TCA scrubber can be made up of several stages such as the one shown in Figure 3.5. In the development to follow it will be assumed that the overall gas side mass transfer coefficients for the spray sections and the packed sections are constant regardless of the position of the section in the column and that the height of the packed section in the fluidized state can be characterized by the height of the packed section without gas flow. Chen and Douglas^[23],

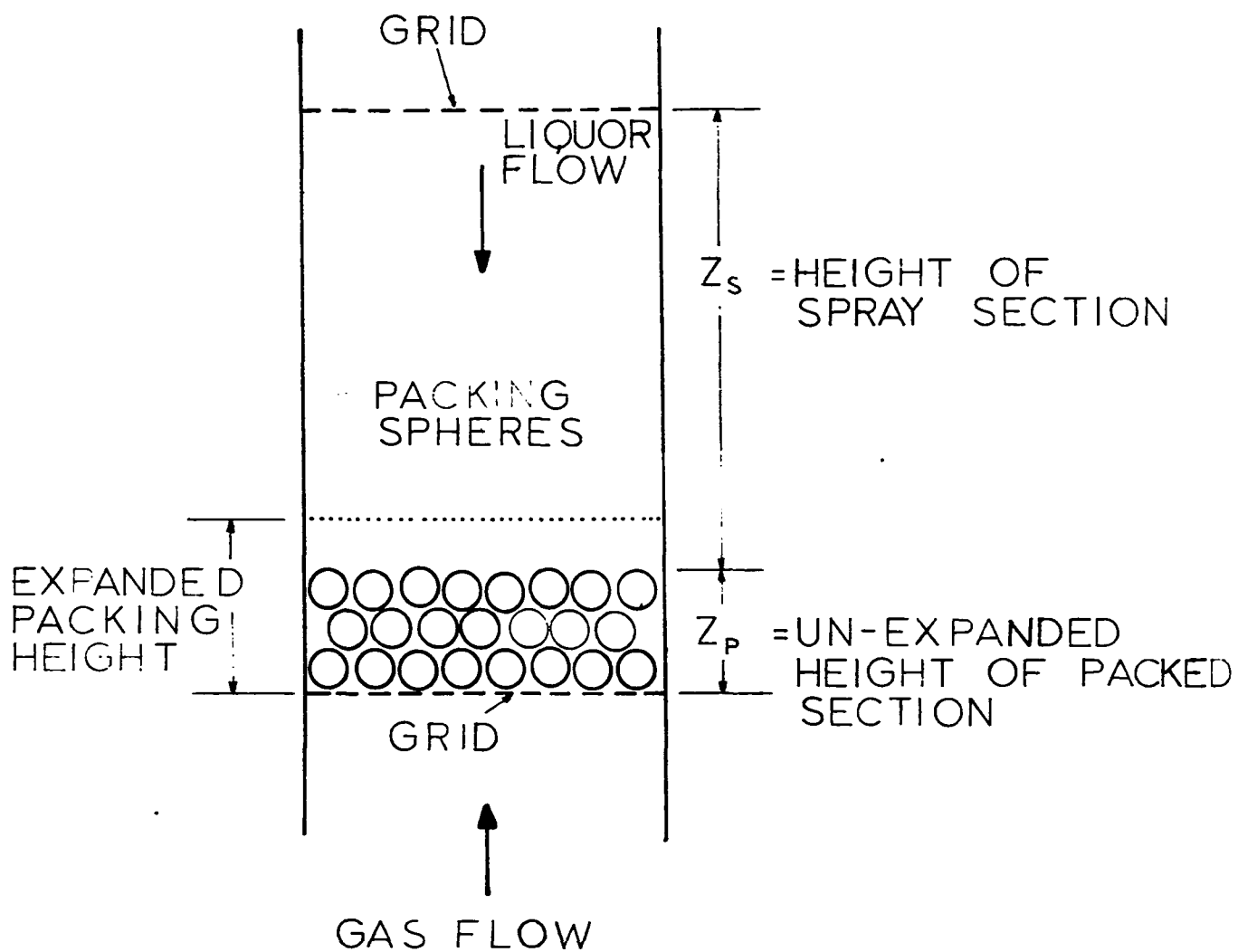


Figure 3.5 An Idealized Stage of a Turbulent Contacting Absorber.

(1968) have reported bed expansion for TCA scrubbers; however, their data was taken for gas velocities substantially lower than the gas velocities of interest in this study.

The integrated mass balance on SO_2 in the TCA scrubber can be written as

$$\frac{G}{P_T} \ln \frac{P_{\text{SO}_2}^{\text{in}}}{P_{\text{SO}_2}^{\text{out}}} = \frac{P}{K_G^a} Z_p + \frac{s}{K_G^a} Z_s \quad (3-15)$$

where $\frac{P}{K_G^a}$, $\frac{s}{K_G^a}$ are the overall gas side mass transfer coefficients in the packed and spray sections of the TCA, respectively, ($\text{gmol}/\text{cm}^3 \text{ atm sec}$),

and Z_p and Z_s are total height of the packed and spray sections of the TCA scrubber, respectively, (cm).

In terms of the ratio of the mass transfer resistance of the gas film to that of the liquid film, Equation (3-15) can be written as

$$\frac{G}{P_T} \ln \frac{P_{\text{SO}_2}^{\text{in}}}{P_{\text{SO}_2}^{\text{out}}} = k_g^P \left(\frac{R_p}{R_p+1} \right) Z_p + k_g^S \left(\frac{R_s}{R_s+1} \right) Z_s \quad (3-16)$$

This follows from Equation (3-10).

Equation (3-16) will be applied to the data reported by Borgwardt (see Table 3.2 for references). These data were obtained from a relatively small TCA scrubber which is shown in Figure 3.3. Only data where the pH of the inlet scrubbing slurry is greater than or equal to 6.6 were considered. At this pH the transfer of SO_2 in the packed section is assumed to be gas film controlled. Examination of Figure

Table 3.2

Range of Data for the EPA/RTP Research TCA Scrubber Used in the Estimation of the Gas Side Mass Transfer Coefficient for the Packed Section of the TCA Scrubber.

Equipment and References	pH	G ($\frac{\text{gmole}}{2 \text{ cm}^2 \text{ sec}}$)	L ($\frac{\text{g}}{2 \text{ cm}^2 \text{ sec}}$)	Z _p (cm)	Inlet P _{SO₂} (ppm)	Mg Concentration (ppm)
EPA/RTP Research	6.6	0.00577	1.373	50.8	~2520	less than 350
TCA Scrubber	6.8	0.01355	3.150			
(Borgwardt ^[12,13,18])						

3.4 shows that this is not the case for the spray section at a pH of 6.6, however, the value of the liquid film mass transfer coefficient in the packed section will be much higher than in the spray section; and thus, the ratio of resistances in the packed section will, in all likelihood, be significantly larger than in the spray section.

Under the above assumption Equation (3-16) becomes

$$\frac{G}{P_T} \ln \frac{p_{SO_2}^{in}}{p_{SO_2}^{out}} = k_g^P a Z_P + k_g^S a \left(\frac{R_S}{1+R_S} \right) Z_S \quad (3-17)$$

Thus using Borgwardt's data for $pH \geq 6.6$, the gas film mass transfer coefficient for physical absorption, $k_g^P a$, can be computed from Equation (3-17). This coefficient as a function of the gas and liquid flow rates is given by

$$k_g^P a = 0.0352 G L^{0.35} \quad (3-18)$$

The range of data from which this coefficient was obtained is given in Table 3.2. It was assumed in the above calculation that the gas film mass transfer coefficient for the Shawnee spray column given by Epstein (Equation (3-11)) was applicable to the spray section of Borgwardt's TCA column.

Epstein has made several reliability runs for the Shawnee TCA scrubber. In these long term tests the pH of the scrubbing slurry, temperature and the liquid and gas flow rates are held almost constant. However, the inlet partial pressure of SO_2 varied. As can be seen in the example of Epstein's data given in Figure 3.6, a decrease in the partial pressure of SO_2 causes a corresponding increase in

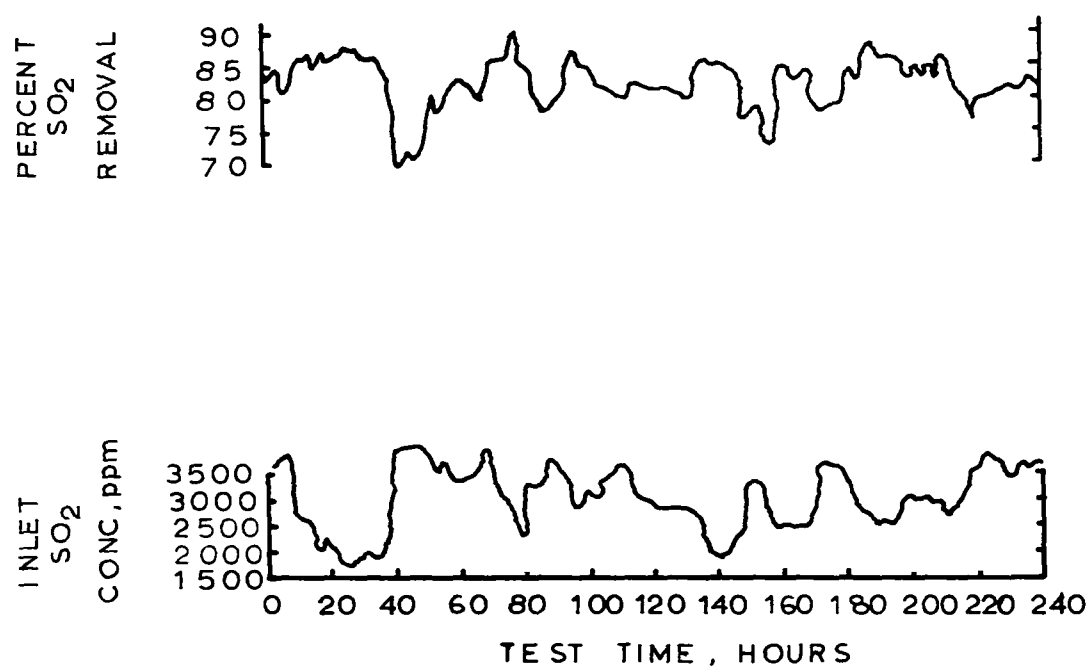


Figure 3.6 Typical Operating Data for the TVA Shawnee TCA Showing the Dependence of the SO₂ Removal Efficiency on the Inlet SO₂ Concentration. (Epstein^[30] Run 525-2A).

the SO_2 absorption efficiency. These data can be utilized to determine the dependency of the ratio of resistances on the SO_2 partial pressure. The ratio of the resistances is computed for the overall TCA column with the spray and packed sections un-segregated using Equations (3-9) and (3-10). The value of the gas film mass transfer coefficient for physical absorption, $k_g a$, used in Equation (3-10) to calculate the overall ratio was calculated from the following relationship:

$$k_g a^{\text{overall}} = k_g^s a \frac{Z_s}{Z_T} + k_g^p a \frac{Z_p}{Z_T} \quad (3-19)$$

where $k_g^s a$ and $k_g^p a$ were evaluated from Equations (3-11) and (3-18) respectively.

The results of these calculations are shown in Figure 3.7. Here \bar{R} , the overall ratio of resistances for the Shawnee TCA, is shown as a function of the inlet SO_2 partial pressure. It can be seen in this figure that the ratio of the resistances can be expressed as

$$\bar{R} = A(\text{pH}) e^{-330P_{\text{SO}_2}} \quad (3-20)$$

Equation (3-20) shows that the overall ratio of resistances is the product of a pH function and a function of the SO_2 partial pressure. The exponential term in Equation (3-20) follows from Figure 3.7 and the pre-exponential pH function has been assumed; although, it is not apparent in Figure 3.7 that the function A is a function of pH. This relationship will be shown below.

In what is to follow it will be assumed that the ratio of the mass transfer resistances of the gas film to that of the liquid film has the form of Equation (3-20) for both the spray and packed

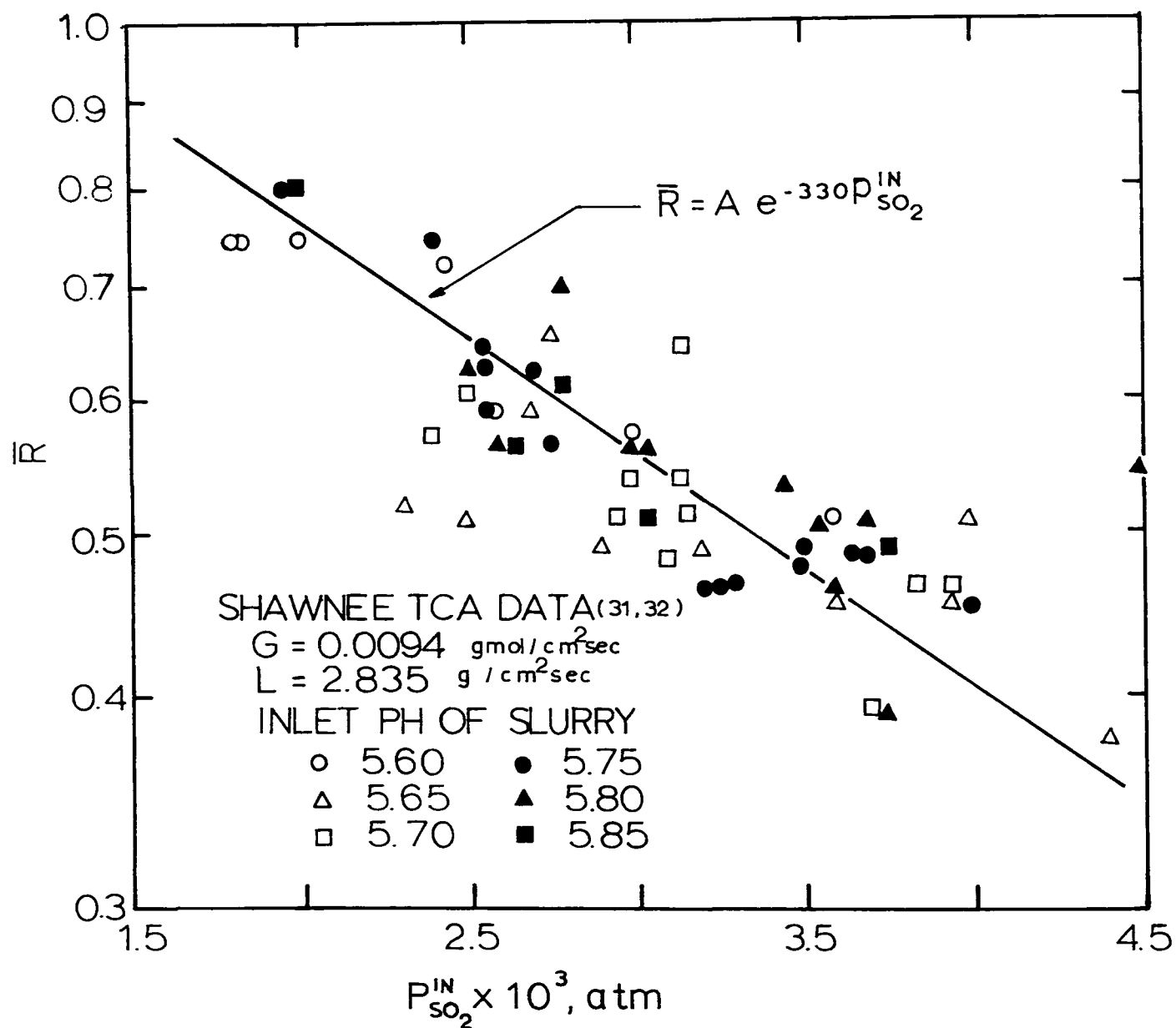


Figure 3.7 The Ratio of the Gas Film to the Liquid Film Mass Transfer Resistance as a Function of the Inlet SO_2 Partial Pressure for the TVA Shawnee TCA.

sections of the TCA. For the Shawnee TCA operating without packing spheres and the spray column with four spray headers the pH function, A , is shown as a function of pH in Figure 3.8.

A new value of the gas film mass transfer coefficient for physical absorption for the packed section of the TCA, k_g^P , can be calculated based on the A function for the spray section given in Figure 3.8. The following equation can be used to calculate the gas film coefficient for the packed section, k_g^P

$$\frac{G}{P_T} \ln \frac{P_{SO_2}^{in}}{P_{SO_2}^{out}} = k_g^P Z_p + k_g^S \left[\frac{1}{330 P_{SO_2}} \frac{1}{1 + \frac{e}{A_s(pH)}} \right] Z_s \quad (3-21)$$

Again Borgwardt's data (see Table 3.2 for references) for the scrubbing of SO_2 with limestone slurries having a pH greater than or equal to 6.6 can be used in conjunction with Equation (3-21) to obtain k_g^P . This coefficient can be expressed as a function of the liquid and gas flow rate as:

$$k_g^P = 0.00220 G^{.47} L^{.51} \quad (3-22)$$

Since a new value of the gas film mass transfer coefficient has been found, the functional dependence of the ratio of resistances on the SO_2 partial pressure should be re-evaluated in a manner similar to that used to obtain the data in Figure 3.7. However, if \bar{R} is recomputed using the value of k_g^P given by Equation (3-22) the slope of the line through the plot of $\log \bar{R}$ versus SO_2 partial pressure is

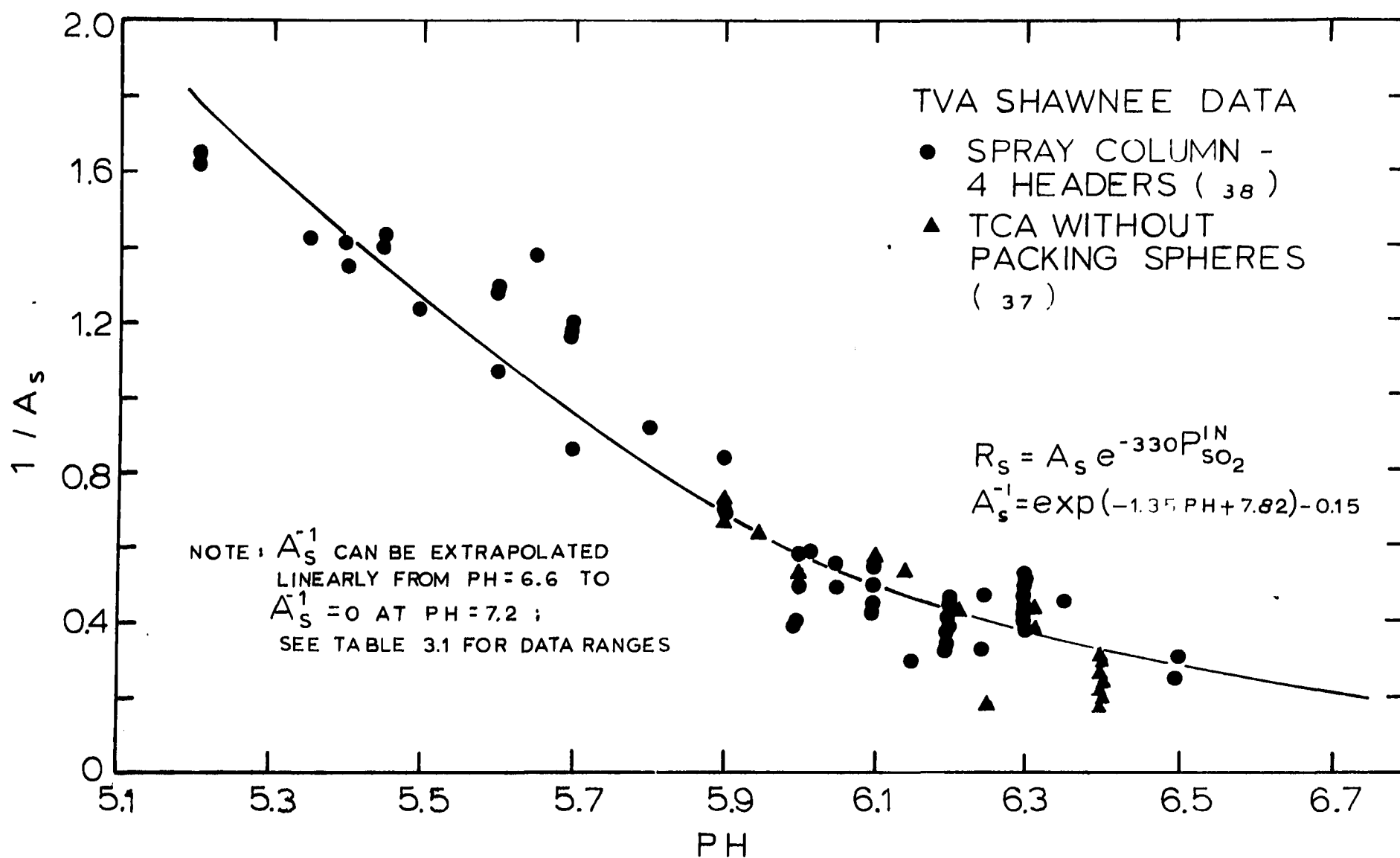


Figure 3.8 The Pre-Exponential Function, A_s , in the Expression for R , the Ratio of Resistance, as a Function of the pH of the Inlet Slurry for the TVA Shawnee TCA Without Spheres and Spray Column. Low Magnesium Concentration ($Mg < 350$ ppm).

approximately the same as that given in Figure 3.7 where \bar{R} was computed based on $k_g^P a$ given by Equation (3-18). The magnitude of the two values of \bar{R} are slightly different however.

The pre-exponential pH function, A , for the packed section of the TCA scrubber can be determined from the data reported by Borgwardt and Epstein (references are given in Table 3.3) using the following equation:

$$\frac{G}{P_T} \ln \frac{P_{SO_2}^{in}}{P_{SO_2}^{out}} = \left[\frac{k_g^P a}{330 P_{SO_2}} \right] Z_p + \left[\frac{k_g^S a}{330 P_{SO_2}} \right] Z_s \quad (3-23)$$

$$\left[1 + \frac{e}{A_p} \right] \quad \left[1 + \frac{e}{A_s} \right]$$

The gas film mass transfer coefficients for the packed section, $k_g^P a$, and the spray section, $k_g^S a$, of the TCA can be determined by Equations (3-22) and (3-11) respectively. Other quantities appearing in Equation (3-23) are evaluated from the experimental data.

The pre-exponential function for the packed section, A_p , is shown in Figure 3.9. Although there is a substantial degree of scatter, the trend of A_p as a function of the slurry pH can be seen. Apparently, within the scatter of the data the function A_p is not dependent on the gas and liquid flow rates. The scatter in Figure 3.9 is probably due in part to using the average value of data, which is reported in ranges, as well as to the normal experimental error associated with data taken from large scale equipment where operating conditions and purity of reagents cannot be carefully controlled. Also in the recycle scrubber-holding tank systems small impurities introduced into the system, such as chlorine, which

Table 3.3

Range of Data for the TVA Shawnee TCA and EPA In-House TCA Used in Determining Λ_p in Figure 3.9.

Equipment and References	pH	G ($\frac{\text{gmole}}{\text{cm}^2 \text{sec}}$)	L ($\frac{\text{g}}{\text{cm}^2 \text{sec}}$)	Inlet Slurry Temperature (°F)	Inlet P_{SO_2} (atm) $\times 10^3$	Total Height of Packing Spheres (cm)
TVA Shawnee TCA	5.2	0.00692	1.382	78	1.775	38.1
[29,30,31]	to	to	to	to	to	
Epstein 32,36,37]	6.3	0.01256	2.835	127	4.4	
EPA In-House TCA	6.6	0.00577	1.373			50.8
	to	to	to	110		to
Borgwardt [12,13,18]	6.8	0.01355	3.15		2.52	76.2

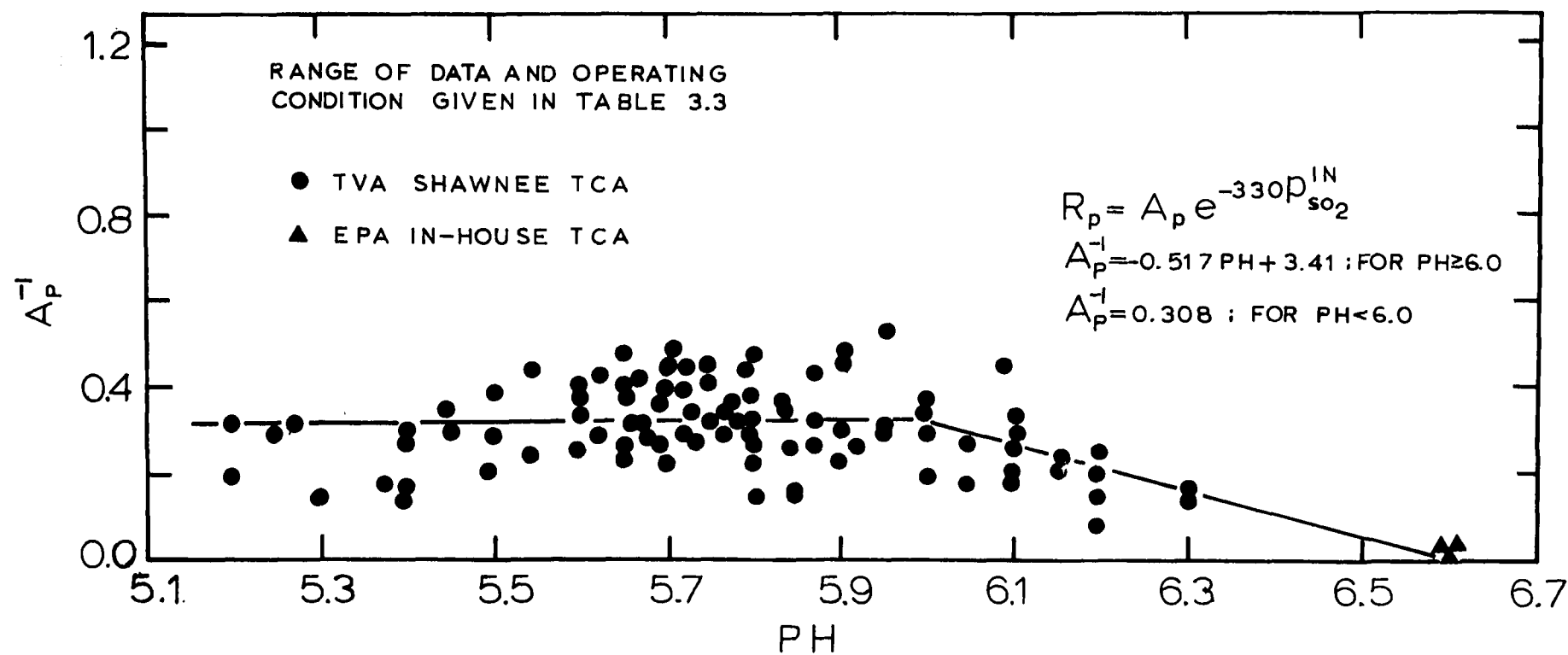


Figure 3.9 The Pre-Exponential Function, A_p , in the Expression for R , the Ratio of Resistances, as a Function of the pH of the Inlet Slurry for the Packed Section of TVA TCA and EPA TCA. Low Magnesium Concentration ($Mg < 350$ ppm).

originates from the coal and is absorbed in the scrubber, have a tendency to build to very high concentration levels thus making a complete analysis of the scrubbing system extremely difficult.

3.2.3 Effect of Magnesium on SO₂ Scrubbing Efficiency

The addition of magnesium oxide to the scrubbing slurry has two major benefits to the operation of limestone wet scrubbers: 1) the addition of magnesium can allow the scrubbing system to operate in the unsaturated mode which prevents calcium sulfate scale formation (see Borgwardt^[22]) and 2) the addition of magnesium improves scrubbing efficiency of the system.

Since the composition of the slurry effects the scrubbing efficiency of the scrubber only through the pre-exponential terms, A_p and A_s , in the expression for R_p and R_s (see Equation (3-20)), it was assumed that the effect of magnesium in the slurry on the scrubbing efficiency could be associated with a change in the pre-exponential factors, A_p and A_s . Thus correction factors, Δ_p and Δ_s , which would take into account the effect of magnesium on the pre-exponential functions, A_p and A_s , respectively, were defined as

$$\Delta_i = \frac{A_i \text{ (without magnesium present)}}{A_i \text{ (with magnesium present)}} \quad (3-24)$$

where $i = s$ or p for the spray and packed section, respectively.

These correction factors to the pre-exponential term for spray and packed section are given in Figures 3.10 and 3.11, respectively.

The value of the pre-exponential factors without magnesium, A_s and A_p , used in Equation (3-24) were calculated using the solid lines

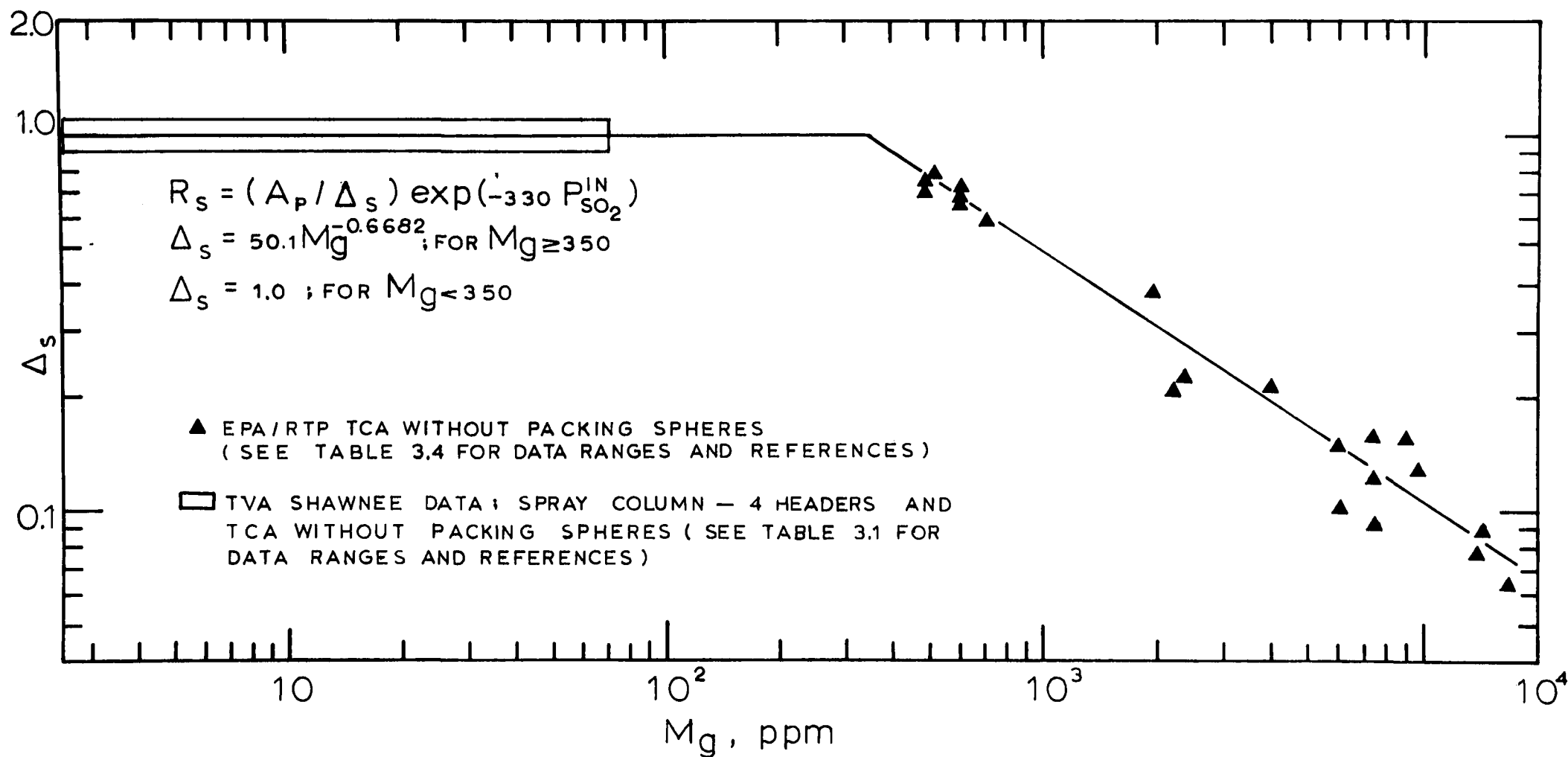


Figure 3.10 The Effect of Magnesium in the Scrubbing Slurry on the Ratio of the Gas to Liquid Mass Transfer Resistances in the Spray Section.

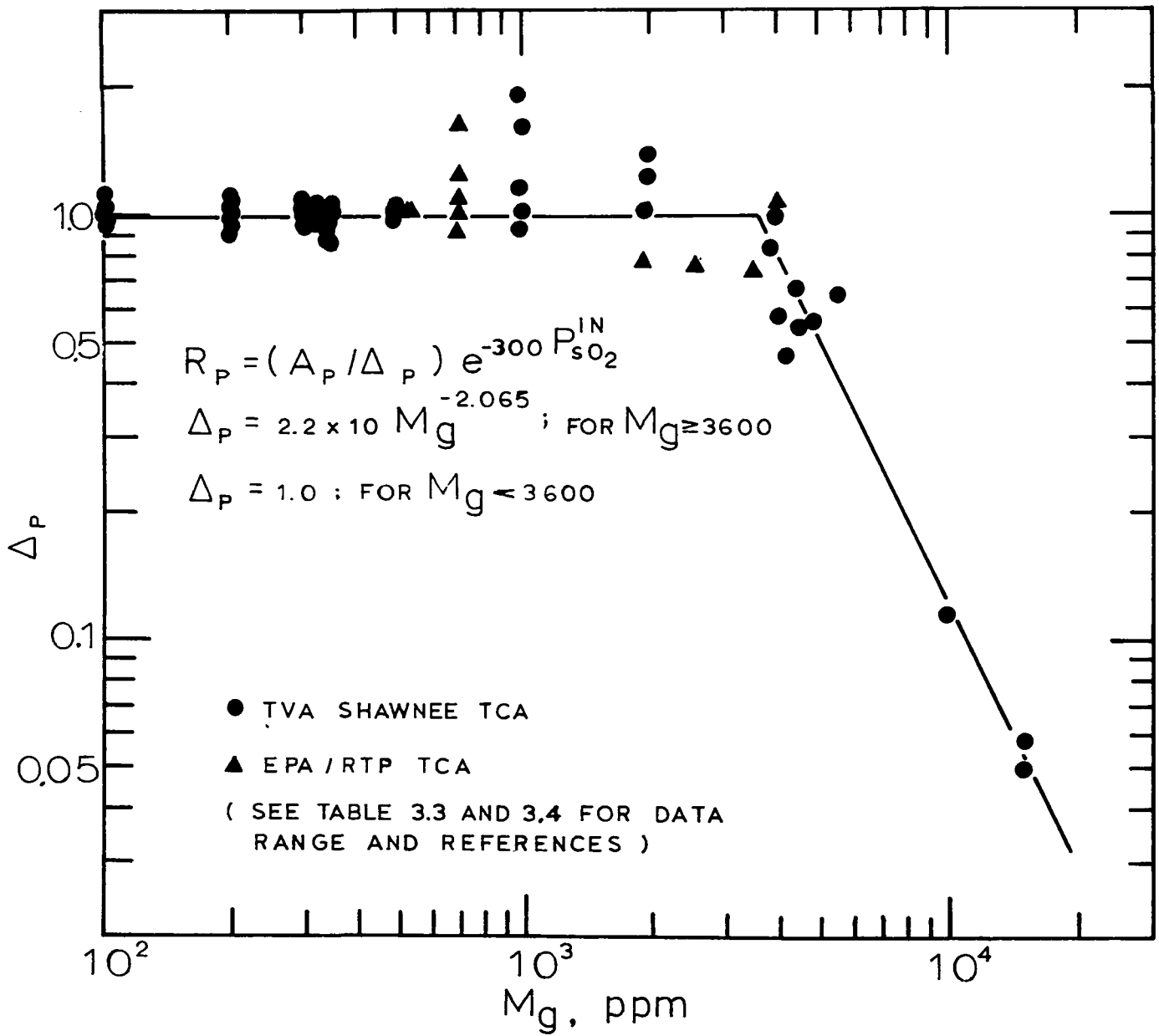


Figure 3.11 The effect of the Magnesium in the Scrubbing Slurry on the Ratio of the Gas to Liquid Mass Transfer Resistances in the Packed Section.

Table 3.4

Range of Scrubber Operating Data Used in Calculating the Effect of Magnesium on the
Pre-Exponential Factor, A.

Equipment and References	pH	G ($\frac{\text{gmole}}{2 \text{ cm}^2 \text{ sec}}$)	L ($\frac{\text{g}}{2 \text{ cm}^2 \text{ sec}}$)	Inlet Slurry Temperature (°F)	Inlet P _{SO₂} (ppm)	Height of Packing (cm)	Magnesium Concentration (ppm)
EPA/RTP Research	5.3	0.0094	1.535		2520		470
TCA Operating without Packing	to	to	to	125	to	none	to
Spheres ^[15,16,20]	6.4	0.0107	3.320		2880		16,700
TVA Shawnee	5.6	0.0094	2.835	116	1900	38.1	450
TCA ^[33,34,35]	to	to	to	to	to	to	to
EPA/RTP Research [10,11,16,17 TCA ^{20]}	6.1	0.0107	3.320	126	3100	76.2	15,000

through the data points of Figures 3.8 and 3.9 respectively. Examination of Figures 3.10 and 3.11 reveals that the interphase transfer of SO_2 from the gas to the scrubbing slurries becomes gas film controlled at high magnesium concentration.

3.3 Simulation of SO_2 Scrubbing With Limestone and Lime Slurries

Table 3.5 summarizes the correlations which can be used to simulate the performance of the TCA and spray column in scrubbing SO_2 from flue gases with limestone slurries. Based on these correlations and the model presented in this study the SO_2 removal efficiencies of the TVA Shawnee TCA and spray column and the EPA/RTP TCA column can be computed fairly accurately and in most cases within 5% accuracy. A comparison of the calculated and observed SO_2 removal efficiencies is shown in Figures 3.12 and 3.13 for the spray and TCA devices, respectively, for limestone scrubbing of SO_2 from flue gases.

Figure 3.14 shows a comparison of the calculated and observed SO_2 removal efficiencies for SO_2 scrubbing with lime slurries. In the case of lime slurries the pH variation across the scrubber is substantial ranging, for example, from 8.0 at the inlet to 4.8 at the outlet. With this large change in pH it is not reasonable to assume that the inlet slurry pH characterizes the slurry composition. However, it has been found that the lime scrubbing system can be simulated fairly accurately by the model developed in this study if the characteristic slurry pH is calculated based on the log mean hydrogen ion concentration:

Table 3.5

Summary of Equations Necessary for Simulating the Performance of the
TVA Shawnee TCA and Spray Column and the EPA In-House TCA

Spray Section	Packed Section
$k_g^s = 0.00134 G^{0.8} L^{0.4} \quad (3-11)$	$k_g^p = 0.00220 G^{0.47} L^{0.51} \quad (3-22)$
$R_s = \left(\frac{A_s}{\Delta_s}\right) e^{-330 P_{SO_2}^{in}}$	$R_p = \left(\frac{A_p}{\Delta_p}\right) e^{-330 P_{SO_2}^{in}}$
A_s given by solid line in Figure 3.8 or by Equation	A_p given by solid line in Figure 3.9 or by Equations
$A_s^{-1} = \exp(-1.35 \text{ pH} + 7.82) - 0.15$	$A_p^{-1} = -0.517 \text{ pH} + 3.41; \text{ for } \text{pH} \geq 6.0$
	$A_p^{-1} = 0.308; \text{ for } \text{pH} \leq 6.0$
Δ_s given by solid line in Figure 3.10 or by Equations	Δ_p given by solid line in Figure 3.11 or by Equations
$\Delta_s = 50.1 \text{ Mg}^{-0.6682}; \text{ for } \text{Mg} \geq 350$	$\Delta_p = 2.2 \times 10^7 \text{ Mg}^{-2.065}; \text{ for } \text{Mg} \geq 3600$
$\Delta_s = 1.0; \text{ for } \text{Mg} < 350$	$\Delta_p = 1.0; \text{ for } \text{Mg} < 3600$
$\bar{K}_G^s = k_g^s R_s / (1 + R_s)$	$\bar{K}_G^p = k_g^p R_p / (1 + R_p)$
$\frac{G}{P_T} \ln \frac{P_{SO_2}^{in}}{P_{SO_2}^{out}} = \bar{K}_G^s Z_s + \bar{K}_G^p Z_p \quad (3-15)$	

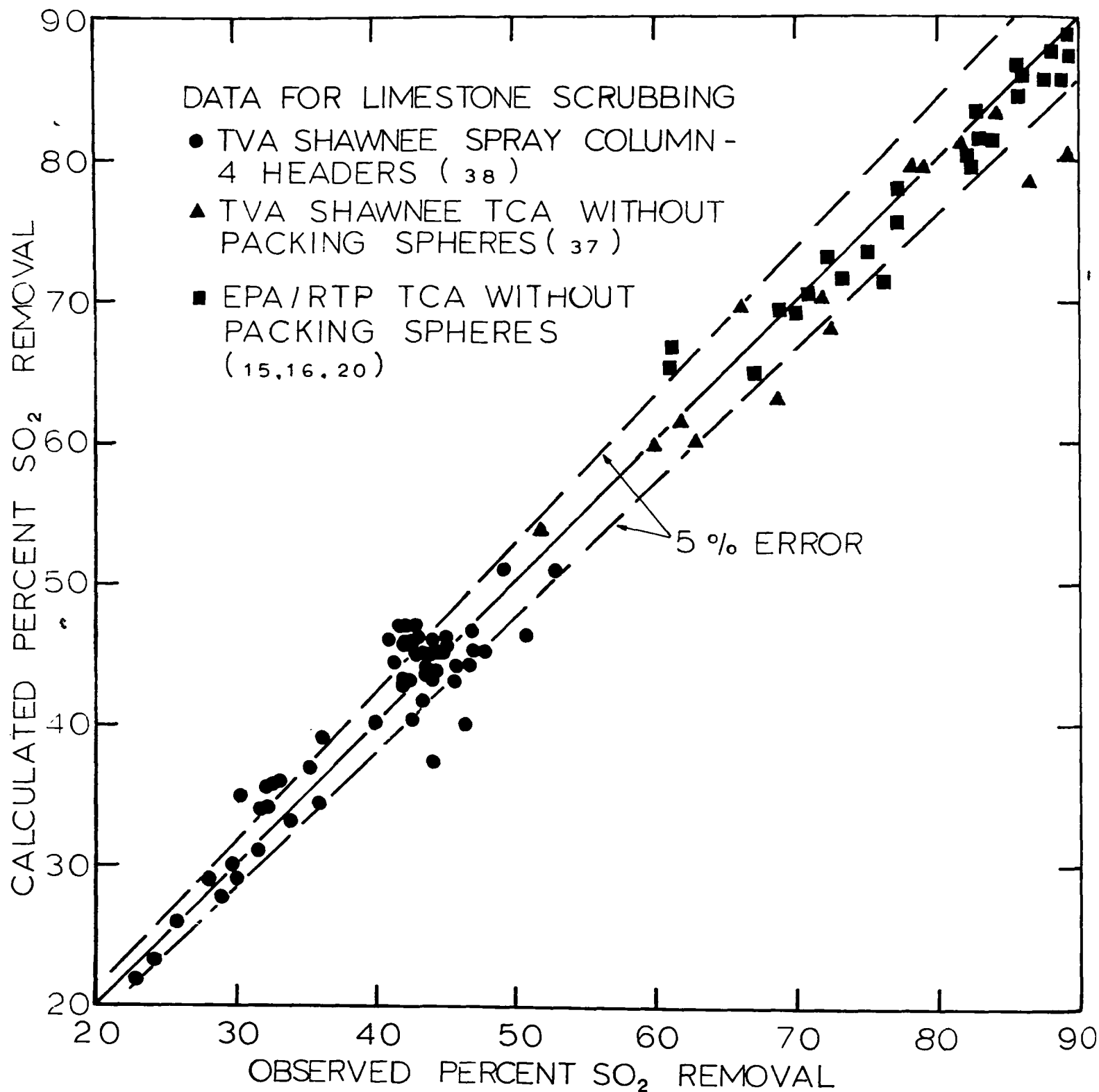


Figure 3.12 Comparison of the Predicted and Observed SO_2 Removal Efficiencies for Spray-Type Devices Using Limestone Slurry as the Scrubbing Medium.

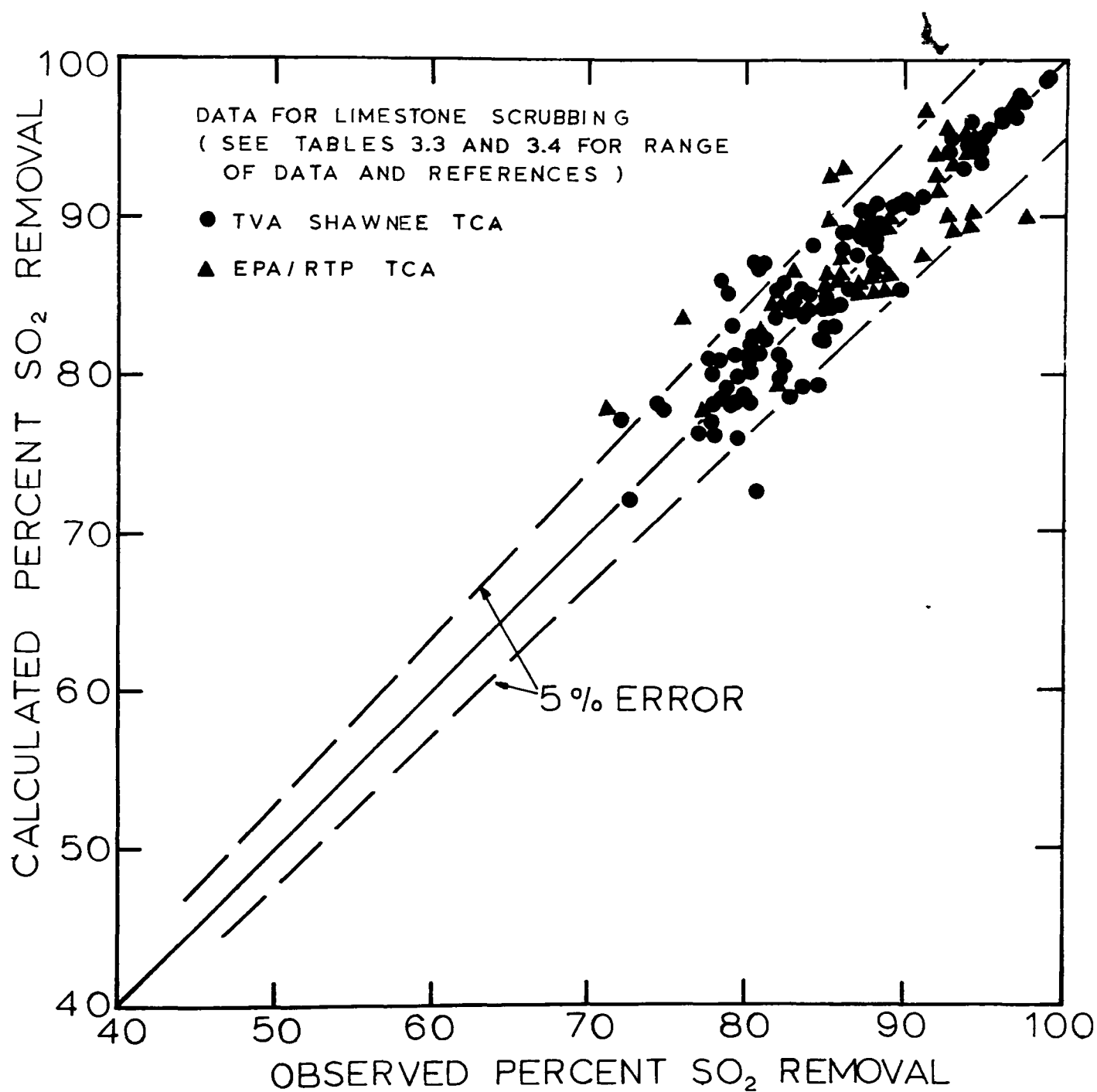


Figure 3.13 Comparison of the Predicted and Observed SO_2 Removal Efficiencies for TCA Scrubbers Using Limestone Slurry as the Scrubbing Medium.

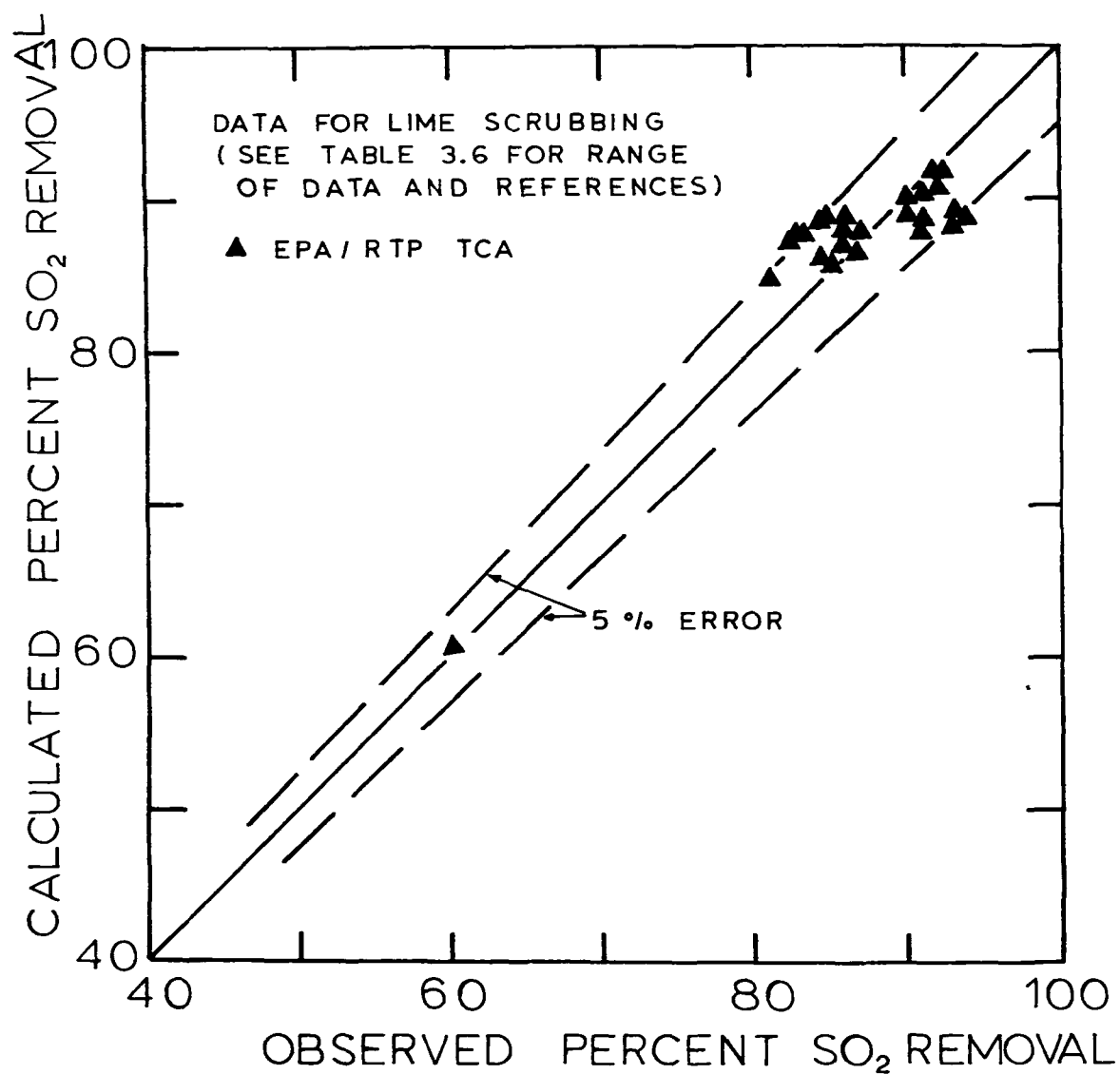


Figure 3.14 Comparison of the Predicted and Observed SO₂ Removal Efficiencies for TCA Scrubber Using Lime Slurry as the Scrubbing Medium.

Table 3.6

Range of Data Used in Constructing Figure 3.14. Data is for the EPA In-House TCA Using Lime Slurries as the Scrubbing Medium

Equipment and References	pH		G ($\frac{\text{gmole}}{2 \text{ cm}^2 \text{ sec}}$)	L ($\frac{\text{g}}{2 \text{ cm}^2 \text{ sec}}$)	Inlet Slurry Temperature (°F)	Inlet P _{SO₂} (ppm)	Height of Packing (cm)	Magnesium Concentration in Liquid (ppm)
EPA In-House TCA	5.7	4.4		3.15		2430	50.8	12
	to	to	0.0136	to	125	to	to	to
Borgwardt [19,21]	9.5	6.0		3.8		2800	76.2	1150

$$pH = 0.562 + \log_{10} \frac{10^{pH_{out}} - 10^{pH_{in}}}{10^{-pH_{in}} - 10^{-pH_{out}}} \quad (3-24)$$

A procedure may be developed by which the pH of the outlet slurry from the scrubber may be calculated from knowledge of the inlet conditions of the scrubber. Then, the model developed in this study for limestone systems may possibly be used to predict the scrubbing efficiency of lime systems. A development of this procedure is presented in Chapter 5.

As shown in Figures 3.12, 3.13 and 3.14, the correlations summarized in Table 3.5 are capable of predicting fairly accurately the scrubbing efficiency of SO₂ scrubbers using limestone slurries as well as lime slurries. These correlations can also provide some insight into the mechanism of SO₂ scrubbing.

Chapter 4
Mechanism of SO₂ Absorption In
Limestone Slurries

4.1 Introduction

Considerable discussion of the overall mechanism of SO₂ absorption into limestone slurries has appeared in the literature and has been recently reviewed by Nannen et al.^[54](1974). Most of the studies reviewed by these authors were concerned with the overall reaction by which SO₂ reacts with limestone (CaCO₃) to form CaSO₃ and CaSO₄. More detailed studies of the absorption of SO₂ into alkaline solutions have been carried out by Bjerle et al.^[7](1972) and Vivian^[65](1973).

Bjerle et al.^[7] experimentally studied the absorption of SO₂ into calcium carbonate slurried with pH's in the range of 8 to 9 in a laminar jet absorber and found that the SO₂ absorption in calcium carbonate slurry was greater than in water due to the instantaneous reaction between absorbed SO₂ and the HCO₃⁻ ion. Furthermore Bjerle et al.^[7] observed that the SO₂ absorption rate into a slurry with a pH of 8.3 and having HCO₃⁻ ion concentration of 0.1 Molar was equal to the SO₂ absorption rate into a 0.1 Molar NaOH solution. Vivian^[65] studied the absorption of SO₂ into lime slurries with pH's in the range from 12 to 13 in a short wetted wall column. He concluded that the SO₂ absorption was enhanced by the instantaneous reaction between absorbed SO₂ and the hydroxyl ion. Based on the observations of Bjerle et al.^[7] and Vivian^[65] it can be hypothesized that there would be a point at which both hydroxyl and bicarbonate ions could have the same

relative importance in the absorption SO_2 into a slurry.

4.2 Reaction Mechanism

By analyzing the correlations presented in the preceding chapter possible mechanism for SO_2 absorption into limestone slurries, which is consistent with the observations of Bjerle et al.^[7] and Vivian^[65] be identified. In this development, absorbed SO_2 as H_2SO_3 is assumed to react instantaneously and irreversibly with some unknown species which has concentration of C_B in the bulk liquid phase.



For this case, the enhancement factor, ϕ , for SO_2 absorption in the liquid film can be written as (see Hatta^[43] (1932)).

$$\phi = 1 + \frac{D_B C_B}{\gamma D_A C_{Ai}} \quad (4-2)$$

where D_A and D_B are the molecular diffusivities of H_2SO_3 and the unknown species B in the liquid phase, respectively, (cm^2/sec), and γ is the stoichiometric factor.

Assuming the diffusivities are equal and the stoichiometric factor is one, Equation (4-2) becomes

$$\phi = 1 + \frac{C_B}{C_{Ai}} \quad (4-3)$$

Substituting this equation into Equation (3-10) gives

$$R = \frac{k_L^o a}{H k_g a} \left[1 + \frac{\bar{C}_B}{C_{Ai}} \right] \quad (4-4)$$

where the bar over the concentration indicates an average concentration.

An expression for the concentration at the gas-liquid interface can be obtained by substituting Equation (4-3) into Equation (3-1) and utilizing Henry's law given by Equation (3-2):

$$\bar{C}_{Ai} = \frac{\bar{P}_{SO_2}}{H(1+R)} \quad (4-5)$$

where \bar{P}_{SO_2} is an average gas phase SO_2 partial pressure.

Substituting Equation (4-5) into Equation (4-4) and subsequent rearrangement gives

$$\frac{1}{R+1} = \frac{Hk_g a}{k_L^o a + Hk_g a} - \frac{k_L^o a \bar{C}_B H}{(k_L^o a + Hk_g a) \bar{P}_{SO_2}} \quad (4-6)$$

Equation (4-6) shows that an estimate of the average concentration of the unknown species, \bar{C}_B , can be calculated from the slope of a linear plot of $1/(R+1)$ versus $1/\bar{P}_{SO_2}$. In the discussion to follow the average gas phase SO_2 partial pressure was chosen as the arithmetic average.

In Figure 4.1 the data reported for the Figure 3.7 for the TVA Shawnee TCA scrubber has been re-plotted in manner suggested by Equation (4-6). The liquid film mass transfer coefficient for physical absorption $k_L^o a$ calculated from the intercept in Figure 4.1 is 0.0403 sec^{-1} and the concentration of the unknown species, \bar{C}_B , calculated from the slope is $0.00053 \text{ gmol/liter}$.

As shown previously the presence of magnesium in the scrubbing slurry has a significant effect on the SO_2 scrubbing efficiency (i.e., an increase in magnesium in the limestone slurry increases SO_2 scrubbing efficiency above that for limestone alone with both slurries having the

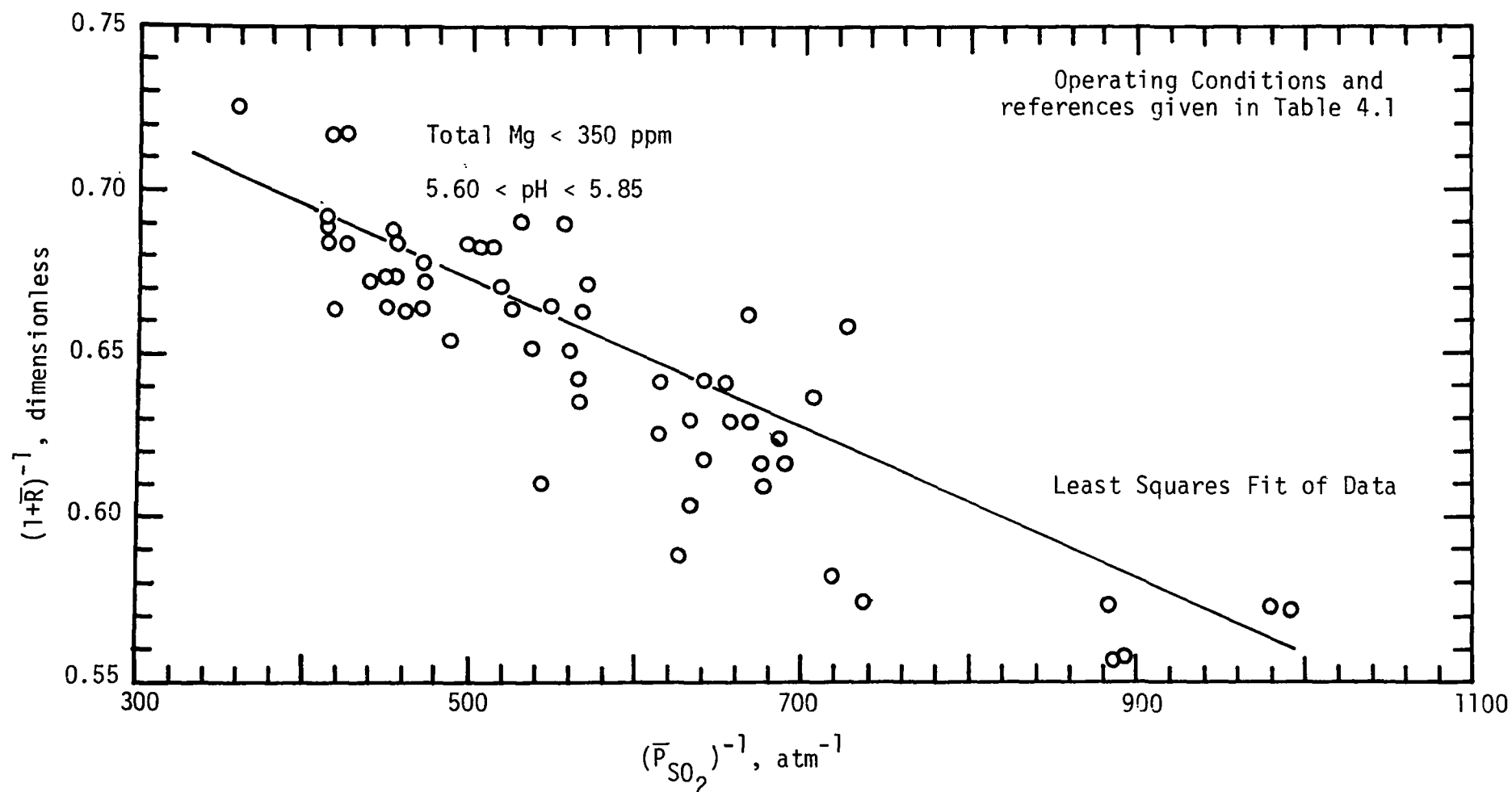


Figure 4.1 The Overall Ratio of the Mass Transfer Resistances as a Function of the Arithmetic Average of the SO₂ Partial Pressure in the Bulk Gas Phase Plotted as Suggested by Equation (4-6). Data from the TVA Shawnee TCA. Low Magnesium Concentration in the Limestone Slurry.

same pH.) The high magnesium concentration data from the TVA Shawnee TCA used in the construction of Figure 3.11 is presented in terms of Equation (4-6) in Figure 4.2. Calculating the liquid film mass transfer coefficient in the absence of chemical reaction, $k_L^{\circ}a$, from the intercept of Figure 4.2 gives a value of 0.0400 sec^{-1} . It can be seen that the agreement between the $k_L^{\circ}a$ calculated from the two sets of data (high and low magnesium concentration) given in Figures 4.1 and 4.2 is amazing. The concentration of the unknown species, C_B , for the high magnesium case is found (from the slope given in Figure 4.2) to be $0.00145 \text{ gmol/liter}$.

It is of interest to compare the calculated concentrations of the unknown specie, C_B , to the selected concentrations predicted from equilibrium. The equilibrium calculations for limestone slurries are based on Radian Corporation Equilibrium Program and have been described in detail by Nelson^[56] (1974). In order to utilize the equilibrium assumption the CO_2 partial pressure in equilibrium with slurry and the pH must be specified.

In the absence of experimental data the CO_2 partial pressure in equilibrium with the slurry is assumed to be equal to the flue gas partial pressure of about 0.12 atm . The specified pH was chosen as the inlet slurry pH to the scrubber.

Table 4.1 gives a comparison of the calculated value of the concentration of the unknown species, \bar{C}_B , (i.e., concentration of the species which reacts instantaneously with H_2SO_3) and the equilibrium concentration of the bicarbonate ion. The agreement between the two for the case of low magnesium is excellent. For the high magnesium

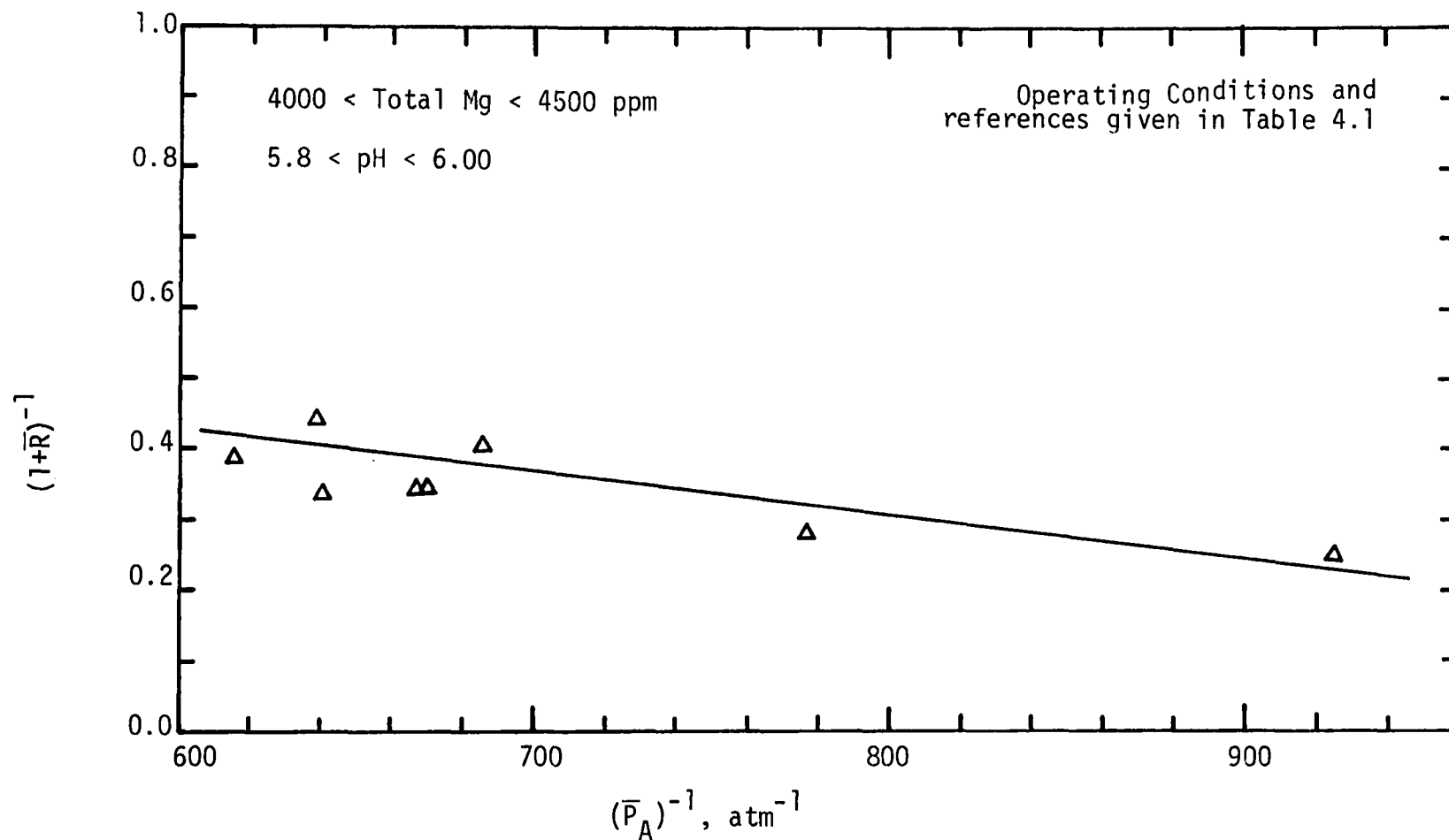


Figure 4.2 The Overall Ratio of Mass Transfer Resistances as a Function of the Arithmetic Average of the SO_2 Partial Pressure in the Bulk Gas Phase Plotted as Suggested by Equation (4-6). Data from the TVA Shawnee TCA. High Magnesium Concentration in the Limestone Slurry.

Table 4.1

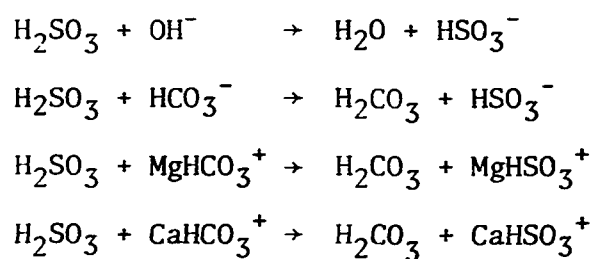
Comparison Between the Calculated Concentration of the Species Which is Hypothesized to Instantaneously and Irreversibly React with Absorbed SO₂ as H₂SO₃ in Limestone Slurries and Selected Species Concentration Predicted from Equilibrium.

Scrubber Type and References		TVA Shawnee TCA Epstein [31,32]	TVA Shawnee TCA Epstein [33]	TVA Shawnee Spray Column Epstein [38]		
Operating Conditions	L(g/cm ² sec)	2.835	2.835	0.652	0.652	0.652
	G(gmol/cm ² sec)	0.0094	0.0094	0.00548	0.00548	0.00548
	Total Mg	< 350	4000 to 4500	< 350	< 350	< 350
	pH inlet	5.60 to 5.85	5.80 to 6.00	5.20 to 5.4	5.60 to 5.8	6.20 to 6.40
Quantities Calculated via Equation (4-6)	Figure Number	4.1	4.2	4.4	4.4	4.4
	k _L ^o a (sec ⁻¹)	0.0403	0.0400	0.00544	0.00544	0.00544
	\bar{C}_B (gmole/liter)	0.000532	0.001450	0.000140	0.000430	0.00188
Equilibrium Concentrations (gmole/liter)	C _{HCO₃⁻}	0.000530	0.001160	0.000220	0.000530	0.002000
	C _{CaHCO₃⁺}	0.000028	0.000084	0.000009	0.000028	0.000075
	C _{MgHCO₃⁺}	0.000015	0.000258	0.000005	0.000014	0.000043
	C _T = $\sum C_i$	0.000573	0.001502	0.000234	0.000573	0.002118

case value of \bar{C}_B is considerably higher than the equilibrium bicarbonate ion concentration. However, if the value of \bar{C}_B is compared to the sum of the bicarbonate and magnesium bicarbonate ion concentrations, good agreement is obtained. The calcium bicarbonate ion would be expected to be chemically similar to the magnesium bicarbonate ion. Therefore, the concentration \bar{C}_B is hypothesized to consist of the sum of four concentrations: (See Appendix B for comments)

$$C_T = C_{OH^-} + C_{HCO_3^-} + C_{MgHCO_3^+} + C_{CaHCO_3^+} \quad (4-7)$$

As can be seen from Table 4.1 the agreement between this total concentration, C_T , and the calculated value of \bar{C}_B is very good. As defined by Equation (4-7), C_T is also consistent with the observations of Bjerle et al.^[7] and Vivian^[65]. An idealization of the concentration profiles in the vicinity of the gas-liquid interface is given in Figure 4.3. The parallel, instantaneous irreversible reactions occurring in the liquid phase would have the form:



The data from the TVA Shawnee spray column used in constructing Figure 3.4 has been re-plotted in Figure 4.4 in the manner suggested by Equation (4-6). A comparison between the concentration, \bar{C}_B , calculated from this figure and the equilibrium total concentration, C_T , is given in Table 4.1; and it can be seen that two concentrations are in fair agreement. One source of error in the agreement could be that the liquid is sprayed into the spray column at four levels

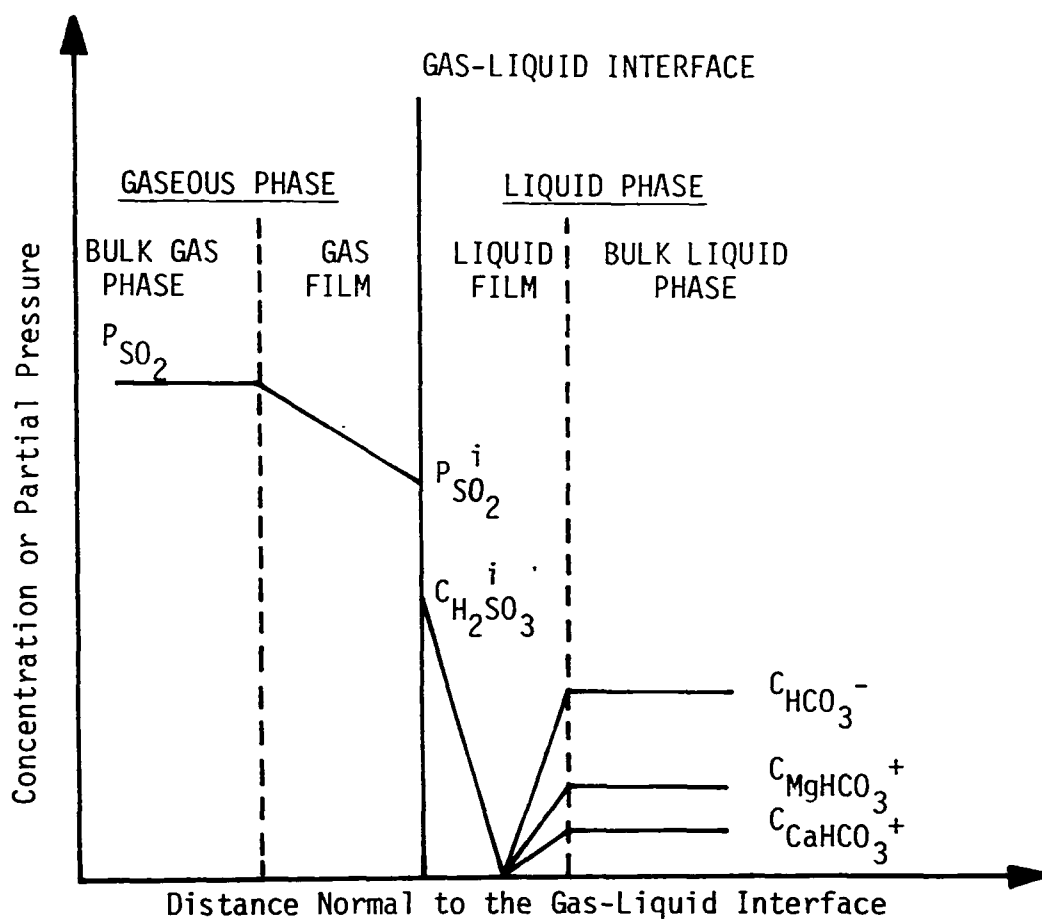


Figure 4.3 Idealization of the Concentration Profiles of Species Important in the Transfer of SO_2 Across the Gas-Liquid Interface and the Chemical Reaction in the Liquid Phase.

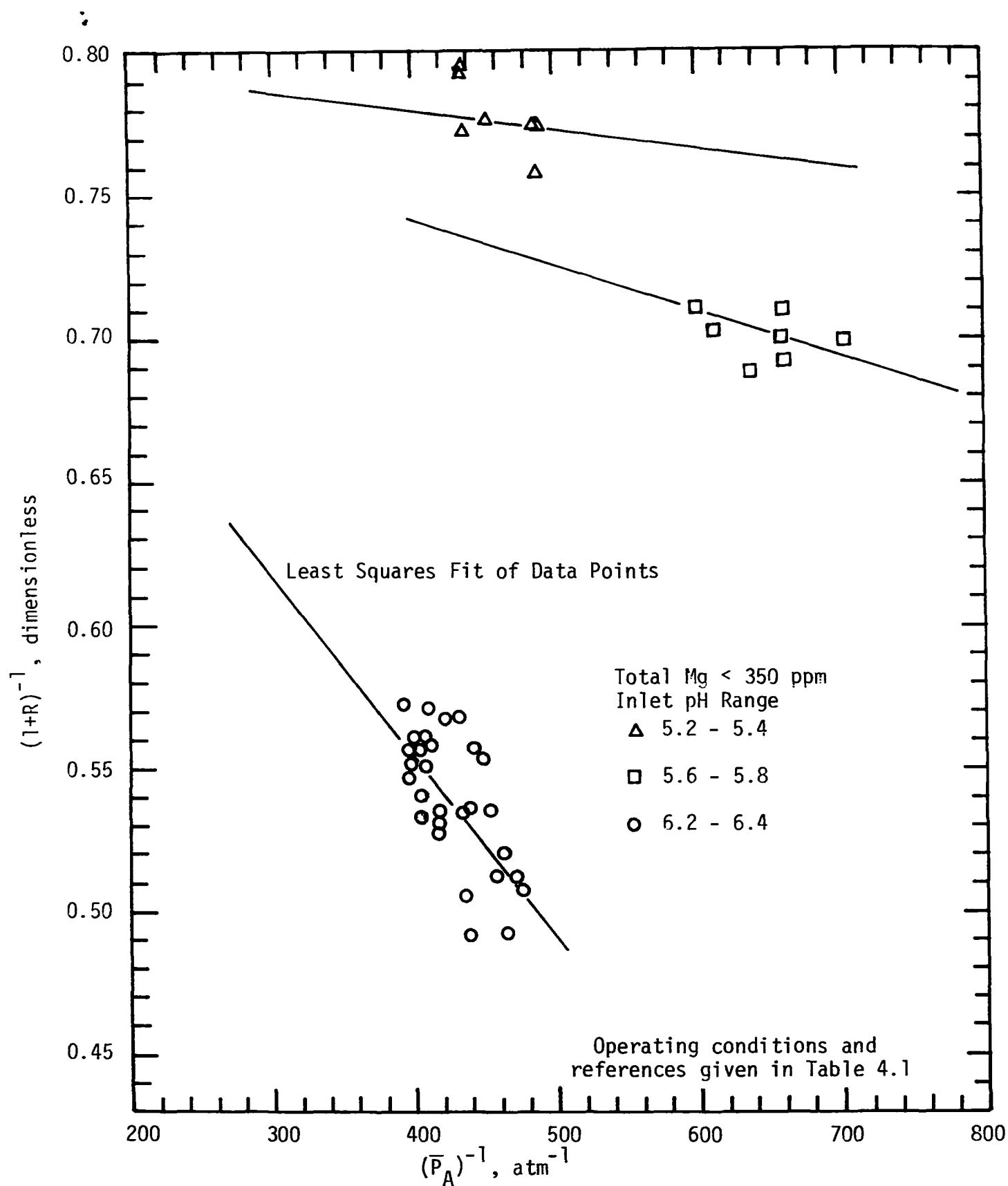


Figure 4.4 The Overall Ratio of Mass Transfer Resistances as a Function of the Arithmetic Average of the SO_2 Partial Pressure in the Bulk Gas Phase Plotted as Suggested by Equation (4-6). Data from the TVA Shawnee Spray Column. Low Magnesium Concentration in the Limestone Slurry.

rather than all the liquid at the top of the column. Since both of the mass transfer coefficients, $k_L^o a$ and $k_g a$, will vary with liquid rate at the various stages of the scrubber, the slopes and intercepts of Figure 4.4 are not strictly correct.

Another source of disagreement between the concentrations \bar{C}_B and C_T given in Table 4.1 is the assumption of the pH and CO_2 partial pressure of the slurry used in the equilibrium calculation as described above. The use of the inlet slurry pH and the flue gas CO_2 partial pressure gives only rough estimates of these quantities since the concentration \bar{C}_B can be viewed as an average concentration and it is not known at which position in the scrubber this concentration applies.

Chapter 5

Analysis of pH for Lime Slurry at the Outlet of the Scrubber

5.1 Introduction

It has been shown in Chapter 3 that the mathematical model, which was developed to describe the absorption of SO_2 by limestone slurries, can be used to simulate the lime slurry scrubber fairly accurately if a characteristic slurry pH corresponding to the log mean hydrogen ion concentration across the scrubber is utilized in the limestone correlations. Hence, in order to be able to estimate the SO_2 scrubbing efficiency in the lime system using the correlations developed for limestone slurries, both the inlet and outlet pH of the scrubbing slurry in the lime system must be known.

The purpose of this chapter is to develop a procedure by which the pH of the outlet slurry from the lime scrubber and the SO_2 removal efficiency of the lime scrubber can be calculated directly from knowledge of the inlet condition of the slurry to the scrubber and scrubber operating conditions. This procedure will make use of the model developed for the limestone system.

For the TCA scrubber, heat transfer is known to occur very rapidly (Barile and Meyer^[5], 1971; Barile et al.^[4], 1974); and the heat capacity of the liquid phase is much greater than that of the gas. Therefore, the system can be assumed to operate isothermally. That is the variation in the liquid and gas temperature throughout the system can be ignored for all practical purposes when the heat of reaction generated in the system is negligibly small. Thus, in

what is to follow, only the mass balances in the scrubber are considered.

5.2 Liquid Phase Material Balance for the Scrubber

The conservation of sulfur, carbon and calcium in the liquid in the scrubber can be written as:

Sulfur

$$M_{SO_2} + L' [S]_{in} + L' S_{s,in} - L' [S]_{out} - L' S_{s,out} = A_s \quad (5-1)$$

Carbon

$$M_{CO_2} + L' [C]_{in} + L' S_{c,in} - L' [C]_{out} - L' S_{c,out} = A_c \quad (5-2)$$

Calcium

$$L' [Ca]_{in} + L' S_{Ca,in} - L' [Ca]_{out} - L' S_{Ca,out} = A_{Ca} \quad (5-3)$$

where:

M_{SO_2} is the absorption rate of SO_2 in the scrubber, mgmole/sec,

M_{CO_2} is the absorption rate of CO_2 in the scrubber, mgmole/sec,

$[k]_i$ is the total liquid phase concentration of species k in the i^{th} stream of the scrubber, mgmole/liter,

$S_{k,i}$ is the total concentration of species k as solid in the i^{th} stream of the scrubber, mgmole/liter,

A_k is the accumulation of species k as solid within the scrubber, mgmole/sec,

and L' is the liquid flow rate, liter/sec.

when:

$i=in,out$ the subscript refers to the inlet and the outlet stream of the scrubber, respectively,

and $k=S,C,Ca$ the symbol k refers to sulfur, carbon and calcium, respectively.

The above equations apply to the steady state operation of the scrubber system, that is, steady state with respect to the liquid concentrations. A rate of scale formation is taken into account through the use of the accumulation terms, A_k .

Steady liquid concentrations may be inconsistent with the steady build up of solids in the scrubber system. For example, it is known that the accumulation of scale in the scrubber can cause an increase in the SO_2 removal which in turn can affect the liquid compositions. However, this process normally takes place slowly and it can be assumed that Equations (5-1) through (5-3) can be applied at each small interval of time. This is equivalent to a quasi-steady state assumption.

Subtracting Equation (5-3) from the sum of Equations (5-1) and (5-2) gives

$$M_{\text{SO}_2} + M_{\text{CO}_2} = L' (\eta_{\text{out}} - \eta_{\text{in}}) \quad (5-4)$$

where:

$$\eta_{\text{out}} = [\text{S}]_{\text{out}} + [\text{C}]_{\text{out}} - [\text{Ca}]_{\text{out}}$$

$$\eta_{\text{in}} = [\text{S}]_{\text{in}} + [\text{C}]_{\text{in}} - [\text{Ca}]_{\text{in}}$$

Here the fact that the solid calcium salts have a one to one correspondence of calcium to sulfur or carbon has been used to eliminate the solid concentrations appearing in Equations (5-1) through (5-3). It can be noted that Equation (5-4) does not contain any solid compositions.

In some cases, solid magnesium salts may also be present in the scrubbing slurry. However, experimental evidence shows that the

amount of solid magnesium salts are usually insignificant in comparison with the amount of solid calcium salts in the scrubbing liquid. Therefore, consideration of the magnesium material balance in the scrubber appears unnecessary.

A further simplification of Equation (5-4) is possible if it is noted that the CO_2 absorption rate, M_{CO_2} , can be ignored for lime slurries. This follows from the fact that the magnitude of the CO_2 absorption rate, M_{CO_2} , evaluated from Equation (5-4) is usually less than 10% of the SO_2 absorption rate, M_{SO_2} (Borgwardt^[19,21], 1974). Consequently, Equation (5-4) for the lime system approximately reduces to

$$M_{\text{SO}_2} = L' (\eta_{\text{out}} - \eta_{\text{in}}) \quad (5-5)$$

In utilizing Equation (5-5) to calculate the scrubbing efficiency and effluent slurry pH of the lime scrubber, this equation must be solved simultaneously along with the expressions developed in Chapter 3 for computing the scrubbing efficiency and the rate of SO_2 absorption, M_{SO_2} . By the methods discussed in Chapter 3, the rate of SO_2 absorption, M_{SO_2} , in the lime scrubber is determined if the inlet and outlet slurry pH, inlet SO_2 partial pressure and operating and scrubber parameters are specified. In the operation of a scrubber, which has no recycle loops, only the inlet slurry pH, inlet SO_2 partial pressure and operating and scrubber parameters may be specified. Therefore, the SO_2 absorption rate can be calculated a priori if the outlet slurry pH from the scrubber can be found. Mathematically this may be expressed as

$$M_{SO_2} = M_{SO_2}(pH_{out}) \quad (5-6)$$

Equations (5-5) and (5-6) give the relationships between the quantities M_{SO_2} , pH_{out} , η_{in} and η_{out} . Therefore, in order to simulate the scrubber, two more relationships must be established or the specification of two variables is necessary. A fortunate circumstance occurs which makes the establishment of two additional relationships a simple matter. The value of η can be related to the pH through chemical equilibrium. Thus,

$$\eta_{in} = E(pH_{in}) \quad (5-7)$$

$$\text{and } \eta_{out} = E(pH_{out}) \quad (5-8)$$

In these equations the symbol E is an operator which relates η to pH through chemical equilibrium. It remains to be shown that the value of η calculated by chemical equilibrium using the experimental pH can closely approximate the experimental value of η . This is done in Figure 5.1. It can be seen from this figure that the agreement between the calculated value of η (or η_{cal}) and the experimental value of η (or η_{exp}) for the slurry at the inlet and outlet of the scrubber is fairly good. The equilibrium relationship between η and pH was calculated using the equilibrium program developed by Radian Corporation. This calculation has been described in detail by Nelson^[56], (1974).

To summarize, the lime scrubber can be simulated by the following sequence of steps:

- 1) Inlet conditions and operational and scrubber parameters are set.

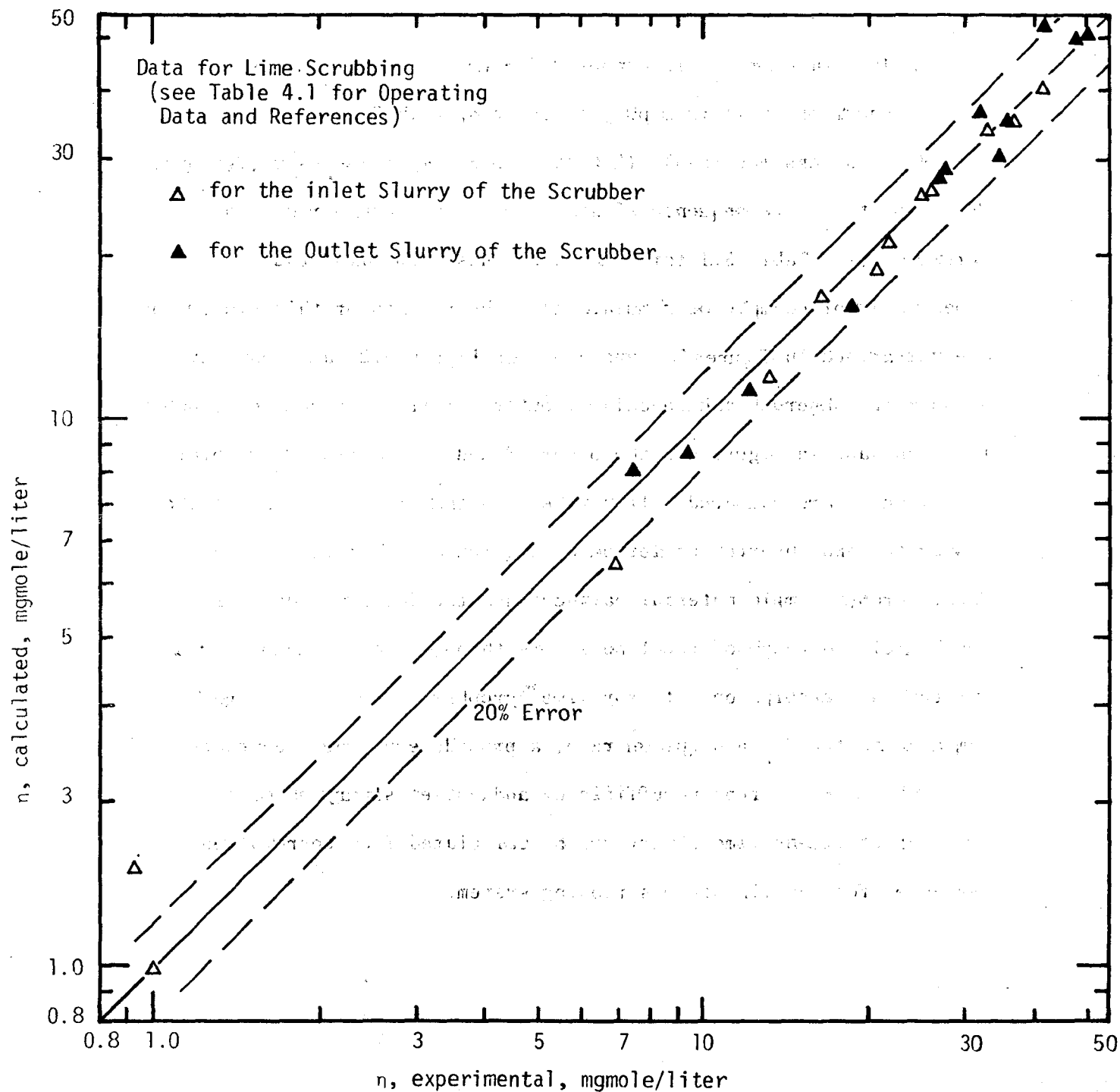


Figure 5.1 Comparison of the Predicted and Observed Values of η for Lime Slurry at the Inlet and Outlet of EPA/RTP TCA Scrubber.

2) The value of η_{in} is computed through chemical equilibrium Equation (5-7) from pH_{in} which is specified.

3) Relationships (5-5), (5-6) and (5-8) are solved simultaneously.

Utilizing the above sequence of steps, the lime scrubber data of Borgwardt (see Table 5.1 for references) has been simulated. (see Appendix A for example of simulation). The results of this simulation are summarized in Figures 5.2 and 5.3. In Figure 5.2, a comparison between the observed and calculated outlet slurry pH from the scrubber is given; and in Figure 5.3 the observed and calculated SO_2 removal efficiencies are compared. It can be seen that the agreement of the calculated and observed outlet pH or SO_2 removal efficiency is good. Thus, through simple material balances and the observations that η can be related to pH of the lime slurry through chemical equilibrium and that CO_2 absorption rate for lime scrubber system is negligible compared to the SO_2 absorption rate, a procedure has been developed by which the SO_2 scrubbing efficiency and outlet slurry pH of a scrubber utilizing lime slurry can be calculated from correlations developed for the limestone scrubbing system.

Table 5.1

Range of Data Used in Constructing Figures 5.1, 5.2 and 5.3. Data is for the EPA In-House TCA
Using Lime Slurries as the Scrubbing Medium

Equipment and References	pH		G	L	Inlet Slurry Temperature (°F)	Inlet P _{SO₂} (ppm)	Height of Packing (cm)	Magnesium Concentration in Liquid (ppm)
	inlet	outlet	($\frac{\text{gmole}}{\text{cm}^2\text{sec}}$)	($\frac{\text{g}}{\text{cm}^2\text{sec}}$)				
EPA In-House TCA	5.7	4.5		3.15		2430	50.8	12
Borgwardt ^[19]	to	to	0.0136	to	125	to	to	to
	9.5	6.0		3.8		2800	76.2	1150

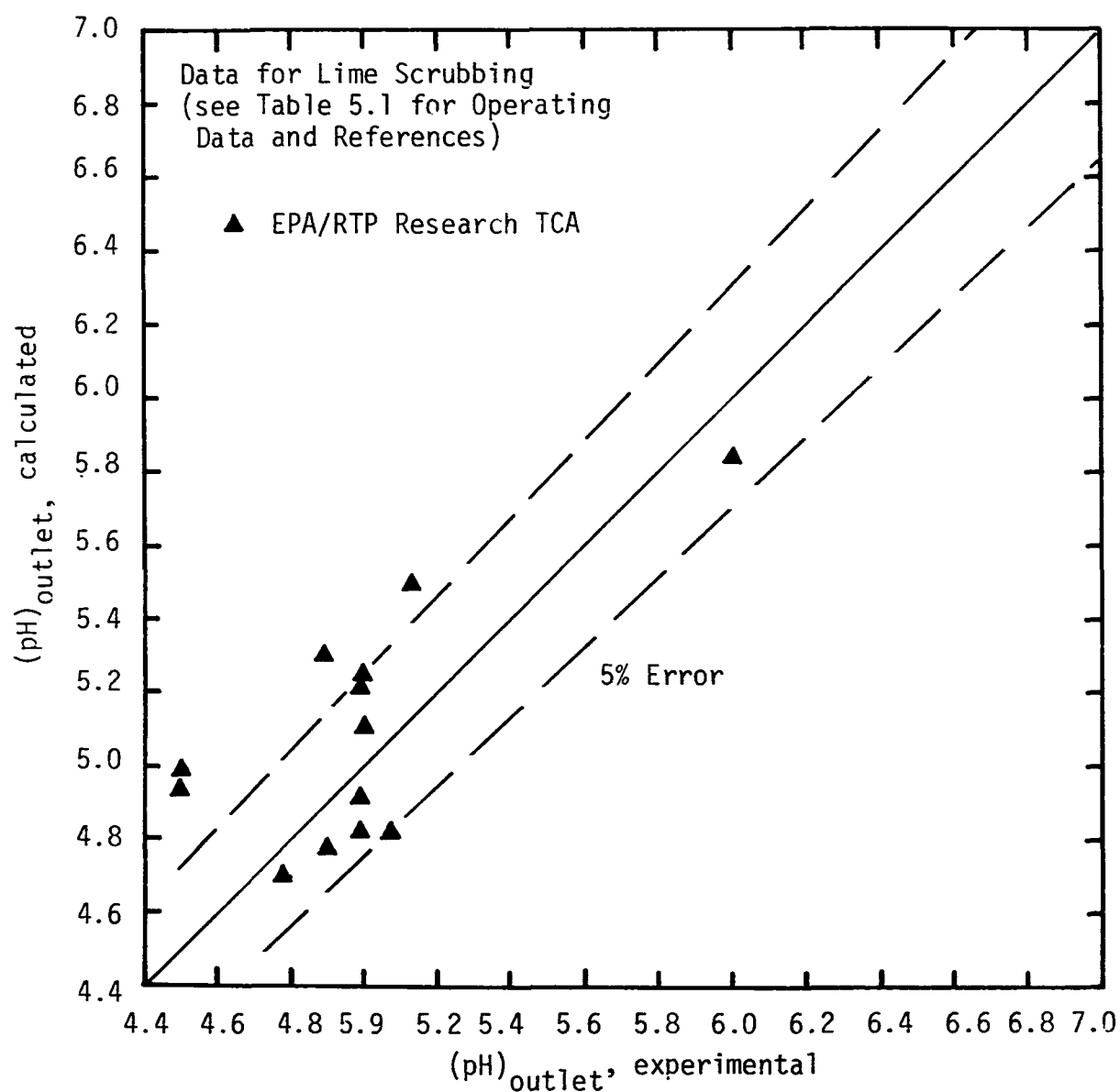


Figure 5.2 Comparison of the Predicted and Observed Outlet Slurry pH for the Simulation of EPA/RTP TCA Scrubber Using Lime Slurry as the Scrubbing Medium.

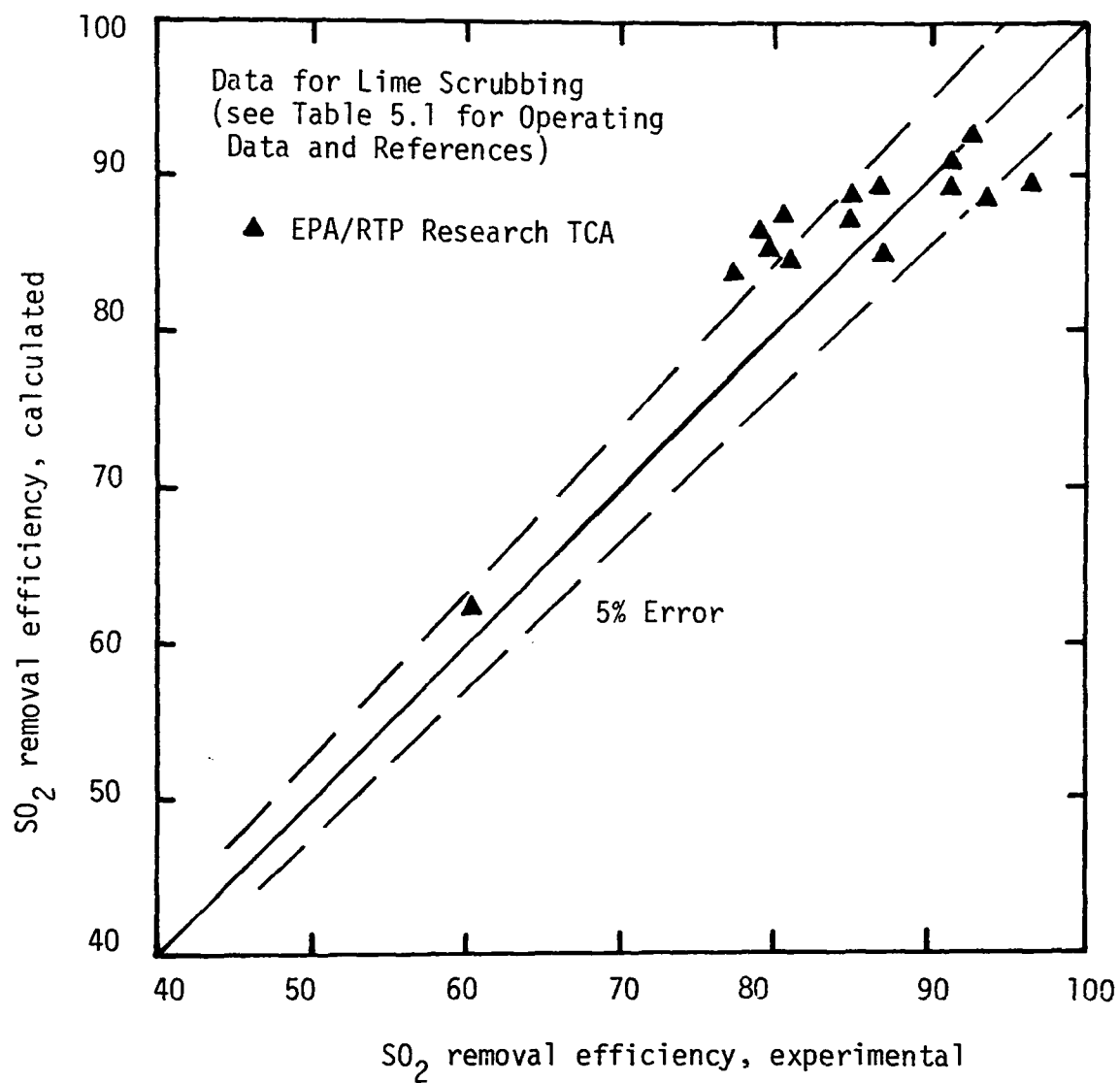


Figure 5.3 Comparison of the Predicted and Observed SO₂ Removal Efficiency for the Simulation of EPA/RTP TCA Scrubber Using Lime Slurry as the Scrubbing Medium.

Chapter 6

Conclusions and Discussion

In this study a mathematical model which can simulate both large and small scale TCA scrubbers used for the scrubbing of SO_2 from flue gases by limestone, limestone-magnesium oxide and lime slurries has been proposed. The parameters which appear in this model have been evaluated from experimental data. The gas film mass transfer coefficients for the spray and packed sections of the TCA were obtained from the literature and calculated from experimental data, respectively. The liquid film resistances for both the spray and packed section were calculated from experimental data and correlated in terms of the ratio of the mass transfer resistance in the gas film to that in the liquid film as a function of inlet pH, magnesium concentration of the scrubbing slurry and inlet partial pressure of SO_2 in the flue gas. Within the accuracy of the experimental data, the ratio of the mass transfer resistances appears to be independent of the gas and liquid flow rates. The temperature dependence of the ratio of resistances was not determined since the experimental data were available only in a narrow range of temperature.

For the data analyzed the chloride concentration in scrubbing liquid ranged from essentially zero to 10,000 parts per million. There did not appear to be any relationship between chloride concentration and SO_2 scrubbing efficiency except through the influence of chloride on the slurry pH.

Although many assumptions were made in the analysis of the limestone scrubbers and scatter of the data can be seen in the derived correlations, these assumptions appear to have given rise to a satisfactory method of simulating the performance of both small and large scale TCA and spray column scrubbers in removing SO_2 from flue gases using limestone, limestone-magnesium oxide or lime slurries as the scrubbing medium. In most cases the calculated SO_2 removal efficiency was within 5% of the experimentally observed efficiency.

The scatter in the data in the figures presented in this study arise from several sources. Probably the most important of these is that many of the data are taken from large scale units where the operating conditions and purity of reagents are difficult to control. Also a substantial number of the data were reported as averages over long periods of operation or reported in ranges and the averages over these ranges were utilized in the analysis.

The liquid film mass transfer resistance was correlated in terms of the ratio of the gas to liquid film resistance because it did not appear possible to separate the liquid film mass transfer coefficient into the enhancement factor and the liquid film mass transfer coefficient for physical absorption. A possible mechanism for SO_2 absorption into limestone slurries has been proposed in this study in which the absorbed SO_2 as H_2SO_3 reacts instantaneously and irreversibly in parallel with OH^- , CaHCO_3^+ , MgHCO_3^+ , and HCO_3^- ions. The physical liquid mass transfer coefficient can be calculated, as shown in this study, by this mechanism. However, sufficient data are not presently available to make this approach practical.

The discussion of the mechanism of SO_2 absorption into limestone magnesium oxide slurries has revealed:

1) that the absorbed SO_2 as H_2SO_3 could possibly react instantaneously and irreversibly with OH^- , HCO_3^- , CaHCO_3^+ and MgHCO_3^+ in parallel reactions.

2) a method by which the liquid phase mass transfer coefficient for physical absorption can be calculated.

The mechanism of SO_2 absorption reported here, with refinement, could be used to model the SO_2 scrubbing efficiency of scrubbers using limestone-magnesium oxide slurries. However, one complicating factor is that the physical liquid film mass transfer coefficient must be known at gas and liquid flow rates encountered in actual scrubbing operations. However, with all the data analyzed in this study only one value of $k_L^o a$ for one pair of gas and liquid rates could be obtained for the TCA scrubber.

For a scrubber which utilizes lime slurries as the scrubbing medium, the SO_2 removal efficiency is shown to be a function of the log mean hydrogen concentration across the scrubber. Therefore, efficiency of the lime scrubber cannot be calculated simply from knowledge of the inlet condition as in the case of the limestone scrubber. A simple procedure has been developed in this study by which the lime system can be simulated with only the inlet conditions being specified. This procedure utilizes the limestone correlations and is based on the observations that the CO_2 absorption rate in the lime scrubber system is very small and that the value of η can be

related to pH of the lime slurry through equilibrium. The procedure has been shown to give reasonable estimates of the SO₂ scrubbing efficiency for the TCA scrubber utilizing lime slurries.

Nomenclature

a	Specific interfacial area available to mass transfer	cm^{-1}
A	Pre-exponential factor in the expression for R defined by Equation (3-20)	Dimensionless
A_k	Accumulation of species k as solid within the scrubber	mgmole/sec
A_p, A_s	Pre-exponential factor in the expression for R for the packed and spray sections, respectively	Dimensionless
C_A	H_2SO_3 concentration in the bulk liquid phase	gmol/cm^3
C_{Ai}	Interfacial H_2SO_3 concentration	gmol/cm^3
\bar{C}_{Ai}	Average interfacial H_2SO_3 concentration	gmol/cm^3
C_B	Concentration of species which react instantaneously and irreversibly with H_2SO_3	gmol/cm^3
C_T	Sum of the OH^- , CaHCO_3^+ , MgHCO_3^+ and HCO_3^- ions	gmol/cm^3
D_A	Molecular diffusivity of specie B in the liquid phase	cm^2/sec
E	An operator, defined by Equations (5-7) and (5-8)	-----
G	Molar gas flow rate based on corss-sectional area of the scrubber	$\text{gmol/cm}^2\text{sec}$
G_g	Molar gas flow rate based on the free projected area of the grid	$\text{gmol/cm}^2\text{sec}$
H	Henry's law constant	$\text{atm cm}^3/\text{gmol}$
$[k]_i$	Total liquid phase concentration of species k in the i^{th} stream of the scrubber	mgmole/liter
k_g	Gas film mass transfer coefficient for physical absorption	$\text{gmol/cm}^2\text{atm sec}$

Nomenclature (continued)

k_L^o	Liquid film mass transfer coefficient for physical absorption	cm/sec
\overline{K}_{Ga}	Average overall gas side mass transfer coefficient	gmol/cm ³ atm sec
\overline{K}_{Ga}^P	Overall gas side mass transfer coefficient for the packed section of the TCA	gmol/cm ³ atm sec
k_{Ga}^P	Gas side mass transfer coefficient for the packed section	gmol/cm ³ atm sec
\overline{K}_{Ga}^S	Overall gas side mass transfer coefficient for the spray section of the TCA	gmol/cm ³ atm sec
k_{Ga}^S	Gas side mass transfer coefficient for the spray section	gmol/cm ³ atm sec
overall k_{Ga}	Gas film mass transfer coefficient defined by Equation (3-19)	gmol/cm ³ atm sec
L	Liquid flow rate based on cross-sectional area of the scrubber	g/cm ² sec
\dot{L}	Liquid flow rate	liter/sec
M_{CO_2}	Absorption rate of CO ₂ in the scrubber	mgmole/sec
M_{SO_2}	Absorption rate of SO ₂ in the scrubber	mgmole/sec
N_{SO_2}	Molar flux of SO ₂	gmol/cm ² sec
ΔP	Pressure drop over the length of the scrubber	in H ₂ O
ΔP_N	Pressure drop <u>without</u> scaling	in H ₂ O
P_{SO_2}	Partial pressure of SO ₂ in the bulk gas phase	atm
\overline{P}_{SO_2}	Average partial pressure of SO ₂ in the bulk gas phase	atm
$P_{SO_2}^i$	Interfacial partial pressure of SO ₂	atm

Nomenclature (continued)

$P_{SO_2}^{in}$	Inlet partial pressure of SO_2 in the bulk gas phase	atm
$P_{SO_2}^{out}$	Outlet partial pressure of SO_2 in the bulk gas phase	atm
$P_{SO_2}^*$	Partial pressure of SO_2 which could be maintained in equilibrium with the bulk liquid phase	atm
P_T	Total pressure	atm
R	Ratio of the gas to liquid film mass transfer resistances	Dimensionless
\bar{R}	Average ratio of mass transfer resistances in TCA	Dimensionless
R_p, R_s	The value of R in the packed and spray sections, respectively	Dimensionless
$S_{k,i}$	Total concentration of species k as solid in the i^{th} stream of the scrubber	mgmole/liter
T	Liquid temperature	$^{\circ}K$
u	Gas mass velocity based on cross-sectional area of the scrubber	$g/cm^2 sec$
u_{mf}	Gas mass velocity u at the minimum fluidization condition	$g/cm^2 sec$
U_B	Linear velocity at the bottom of the scrubber with scale present	cm/sec
U_{BN}	Linear velocity at the bottom of the scrubber without scale present	cm/sec
z	Height measured from gas inlet	cm
ΔZ	Difference between height Z_2 and Z_1	cm
Z_T	Total height of the transfer region	cm
Z_i	Height of the i^{th} position	cm

Z_p	Height of the packed section in the TCA	cm
Z_s	Height of the spray section in the TCA	cm

Greek Symbols

ϕ	Enhancement factor for mass transfer in the liquid film due to chemical reaction	Dimensionless
$\bar{\phi}$	Average enhancement factor	Dimensionless
γ	Stoichiometric factor	Dimensionless
Δ_s, Δ_p	Magnesium correction factor for A_s and A_p	Dimensionless
η_i	$[S]_i + [C]_i - [Ca]_i$	mgmole/liter

Bibliography

1. Ando, J., paper presented in Symposium on Flue Gas Desulfurization, Atlanta, Georgia, (1974).
2. Atsukawa, M., Sangyo Kankyo Kogaku (Japan), 44, 23 (1965).
3. Balabekov, O. S., Tarat Romankov, E. Ya., and Mikhalev, M. F., Trans. Zhur. Prikladnoi Khim., 42, (7), 1540, (1969).
4. Barile, R. G., Dengler, J. L. and Hertwig, T. A., A.I.Ch.E. Symposium Series, 70, (138), 154, (1974).
5. Barile, R. G., and Meyer, D. W., Chem. Eng. Progr. Symp. Ser., 67, (119), 134, (1971).
6. Berkowitz, J. B., Evaluation of Problems Related to Scaling in Limestone Wet Scrubbing, report prepared by ADL for the EPA, April, (1973).
7. Bjerle, I., Bengtsson, S. and Farnkvist, K. Chem. Eng. Sci., 27, 1853 (1972).
8. Blyakher, I. G., Zhivaikin, L. Ya and Yurovskaya, N. A., International Chem. Eng., 7 (3), 485, (1967).
9. Boll, R. H., paper presented at Lime/Limestone Wet Scrubbing Symposium, Pensacola, Florida, (March 16-20, 1970).
10. Borgwardt, R., Limestone Scrubbing of SO₂ at EPA Pilot Plant, Report No. 1, (August, 1972).
11. Borgwardt, R., *ibid.*, Report No. 2 (September, 1972).
12. Borgwardt, R., *ibid.*, Report No. 3 (October, 1972).
13. Borgwardt, R., *ibid.*, Report No. 4 (November, 1972).
14. Borgwardt, R., *ibid.*, Report No. 6 (January, 1973).
15. Borgwardt, R., *ibid.*, Report No. 7 (February, 1973).
16. Borgwardt, R., *ibid.*, Report No. 11 (June, 1973).
17. Borgwardt, R., *ibid.*, Report No. 12 (July, 1973).
18. Borgwardt, R., *ibid.*, Report No. 14 (January, 1974).
19. Borgwardt, R., *ibid.*, Report No. 15 (February, 1974).

Bibliography (Continued)

20. Borgwardt, R., *ibid.*, Report No. 16 (June, 1974).
21. Borgwardt, R., *ibid.*, Report No. 17 (July, 1974).
22. Borgwardt, R., paper presented at the EPA Flue Gas Desulfurization Symposium, Atlanta, Georgia (November 4-7, 1974).
23. Chen, B. H. and Douglas, W. J. M., *Can. J. Chem. Eng.*, 46, 245, (1968).
24. Chen, B. H., and Douglas, W. J. M., *Can. J. Chem. Eng.*, 47, 113, (1969).
25. Cheremisinoff, P. N., and Fellman, R. T., *Power Eng.*, 54, (October, 1974).
26. Devitt, T. W., and Zada, F. K., paper presented in Symposium on Flue Gas Desulfurization, Atlanta, Georgia, (1974).
27. Douglas, H. R., Snider, I. W. A. and Tomlinson, II, G. H., *Chem. Eng. Prog.*, 59, (12), 85, (1963).
28. Douglas, W. J. M., *Chem. Eng. Prog.*, 60, (7), 66, (1964).
29. Epstein, M., EPA Alkali Scrubbing Test Facility at the TVA Shawnee Power Plant, Bechtel progress report prepared for the EPA for July 1, 1973 to August 1, 1973 (August 31, 1973).
30. Epstein, M., *ibid.*, progress report for October 1, 1973 to November 1, 1973 (November 30, 1973).
31. Epstein, M., *ibid.*, progress report for December 1, 1974 to January 1, 1974 (January 31, 1974).
32. Epstein, M., *ibid.*, progress report for January 1, 1974 to February 1, 1974 (February 28, 1974).
33. Epstein, M., *ibid.*, progress report for May 1, 1974 to June 1, 1974 (June 30, 1974).
34. Epstein, M., *ibid.*, progress report for June 1, 1974 to July 1, 1974 (July 31, 1974).
35. Epstein, M., *ibid.*, progress report for July 1, 1974 to August 1, 1974 (August 31, 1974).

Bibliography (Continued)

36. Epstein, M., EPA Alkali Scrubbing Test Facility: Limestone Wet Scrubbing Test Results, report prepared by Bechtel for the EPA (January, 1974).
37. Epstein, M., EPA Alkali Scrubbing Test Facility: Sodium Carbonate and Limestone Test Results, report prepared by Bechtel for the EPA (August, 1973).
38. Epstein, M., Sybert, L., Wang, S. C., Leivo, C. C., Princiotta, F. T., paper presented at the 66th Annual Meeting of the A.I.Ch.E., Philadelphia, Pennsylvania, (November, 1973).
39. Gel'perin, N. I., Savchenko, V. I., Ksenzenko, B. I., Grishko, V. Z., and Dianov, E. A., *Khimicheskoe Promyshlennost*, 11, (1965).
40. Gel'perin, N. I., Grisko, V. Z., Savchenko, V. I., and Shchedro, V. M., *Chem. Petrol. Eng.*, (1), 36, (1966).
41. Gel'perin, N. I., Savchenko, V. I., and Grisko, V. Z., *Teor. Osn, Khim. Tekhnol.*, 2, (1), 76, (1968).
42. Gleason, R. J., paper presented at the Second International Lime/Limestone Wet Scrubbing Symposium, New Orleans, Louisiana (November 8-12, 1971).
43. Hatta, S., *Techol. Reports Tohoku Imp. Univ.*, 10, 119 (1932).
44. Johnstone, H. F., and Silox, H. E., *Ind. Eng. Chem.*, 39, 808, (1947).
45. Johnstone, H. F., and Single, A. D., *Ind.Eng. Chem.*, 29, 288, (1937).
46. Johnstone, H. F., and Williams, G. C., *Ind. Eng. Chem.*, 31, 993, (1939).
47. Khanna, R. T., Ph.D. Thesis, McGill Univ., Canada, (1971).
48. Kito, M., Shimada, M., Sakai, T. Sugiyama, S., and Wen, C. Y., paper to be presented at Engineering Foundation Conferences, California, (June, 1975).
49. Kulbach, A. W., *Chem. Eng. Progr. Symp. Ser.*, 57, No. 35, (1961).
50. Levsh, I. P. Krainev, N. I., and Niyazov, M. I., *Uzb. Khim. Zh.*, 5, 72, (1967).

Bibliography (Continued)

51. Levsh, I. P. Krainev, N. I., and Niyazov, M. I., International Chem. Eng., 8, (4), 610, (1968).
52. McMichael, W. J., Fan, L. S. and Wen, C. Y., paper presented at A.I.Ch.E. Meeting, Houston, Texas, (March 16-20, 1975).
53. Nakagawa, S., Seisan to Gijutsu (Japan), 5, 33, (1964).
54. Nannen, L. W., R. E. West and F. Kreith, J. Air. Poll. Control Association, 24, 29 (1974).
55. "New Floating Bed Scrubber Won't Plug", Chem. Eng., 66, 106, (December 14, 1959).
56. Nelson, R. D., Jr., M.S. Thesis, West Virginia University, Morgantown, West Virginia (1974).
57. O'Neill, B. K., Nicklin, D. J., Morgan, N. J., and Leung, L. S., Canadian J. Chem. Eng., 50, 595, (1972).
58. Potts, J. M., Slack, A. V., and Hatfield, J. D., paper presented at Second International Lime/Limestone Wet Scrubbing Symposium, New Orleans, LA, (November 8-12, 1971).
59. Slack, A. V., Falkenberry, H. L., and Harrington, R. E., J. Air Poll. Control Association, 22, 159, (1972).
60. Strom, S. S., and Downs, W., paper presented at A.I.Ch.E. Meeting, Philadelphia, Pennsylvania, (November 11-15, 1973).
61. Takahashi, T., and Akagi, Y., Memoirs of the School of Eng., Okayama Univ., 3, 51, (1968).
62. Takahashi, T. and Fan, L. T., Removal of Sulfur Dioxide from Waste and Exhaust Gases, Report 12, Institute for Systems Design and Optimization, Kansas State University, Manhattan, Kansas, (1969).
63. Tichy, J., Wong, A., and Douglas, W. J. M., Can. J. Chem. Eng., 50, 215, (1972).
64. Tichy, J., and Douglas, W. J. M., Can. J. Chem. Eng., 51, 618 (1973).
65. Vivian, J. E., The Absorption of SO₂ into Lime Slurries: An Investigation of Absorption Rates and Kinetics, report prepared for the HEW Dept., (September, 1973).

Bibliography (Continued)

66. Weir, Jr., A., paper presented in Symposium on Flue Gas Desulfurization, Atlanta, Georgia, (1974).
67. Wen, C. Y., Wet Scrubber Study, report prepared by West Virginia University for the EPA, Report No. 35 (December, 1973).
68. Yagisawa, and Hayashi, Ryuan, (Japan), 14, 167, (1961).

Appendix A

Numerical Example of the Simulation of EPA/RTP TCA Scrubbers Using Lime Slurry as the Scrubbing Medium

The simulation of the lime scrubber consists of the following sequence of steps:

- 1) Inlet conditions and operation and scrubber parameters are set.
- 2) The value of η_{in} is computed through chemical equilibrium Equation (5-7) from pH_{in} which is specified.
- 3) Relationships (5-5), (5-6) and (5-8) are solved simultaneously.

A numerical example is provided in this Appendix to carry out the simulation of the EPA/RTP TCA scrubber using lime slurry as the scrubbing medium. This simulation follows the sequence of steps given above. The inlet conditions and operation and scrubber parameters are given in Table B.1. The value of η is computed through chemical equilibrium computer program (Nelson^[56], 1974) by specifying the following experimental values for parameters:

Temperature = 125°F

Maximum CO₂ pressure = 0.12 atm

Total Sulfate concentration in the liquid phase = 37.25 mgmole/
liter

Total Magnesium concentration in the liquid phase = 22.75
mgmole/liter

Total Chloride concentration in the liquid phase = 0.0 mgmole/liter
and desirable pH.

The value of η as a function of pH computed from the above described chemical equilibrium computer program is shown in Figure B.1 where the inlet conditions for pH and η are shown. A series of trial and error procedures are involved in solving

Table A.1

Operating Conditions and Reference for the Example Given in Appendix B. Data for the EPA In-House TCA Using Lime Slurries as the Scrubbing Medium

Equipment and References	pH		G	L	Inlet Slurry Temperature (°F)	Inlet P _{SO₂} (ppm)	Height of Packing (cm)	Magnesium Concentration in Liquid (ppm)
	inlet	outlet	($\frac{\text{gmole}}{2 \text{ cm}^2 \text{ sec}}$)	($\frac{\text{g}}{2 \text{ cm}^2 \text{ sec}}$)				
EPA In-House TCA								
Borgwardt ^[19]	6.1	4.9	0.0136	3.15	125	2800	76.2	546

Equations (5-5), (5-6) and (5-8) simultaneously to obtain solutions of M_{SO_2} , η_{out} and pH_{out} . These procedures in terms of numerical solutions are shown in the subsequent development for this example.

- 1) Assume pH_{out} (4.9) to calculate SO_2 removal efficiency (86%) via scrubber model as summarized in Table 3.5.
- 2) Compute the value for M_{SO_2}/L' (9.52 mgmole/liter) from the SO_2 removal efficiency as obtained from step (1) and then, calculate η_{out} (35.52 mgmole/liter) via Equation (5-5). Subsequently, pH_{out} (4.80) can be found via Equation (5-5). Subsequently, Figure B.1. New value of SO_2 removal efficiency (85.5%) can, therefore, be calculated based on the new value of pH_{out} (4.80).
- 3) Compare pH_{out} (4.80) with the assumed value of pH_{out} (4.90) to check if it meets the desirable convergent criterion. The same check applies to the SO_2 removal efficiency.
- 4) If both pH_{out} and SO_2 removal efficiency meet the desirable convergent criteria, the calculation is completed. Otherwise, iteration proceeds from step (1) with new value (4.80) replaced for pH_{out} .

These procedures reveal the following results for this example:

$$\text{pH}_{\text{out}} = 4.80$$

$$\text{SO}_2 \text{ removal efficiency} = 85.5\%.$$

where the experimental observed values for this example are:

$$\text{pH}_{\text{out}} = 4.90$$

$$\text{SO}_2 \text{ removal efficiency} = 81\%.$$

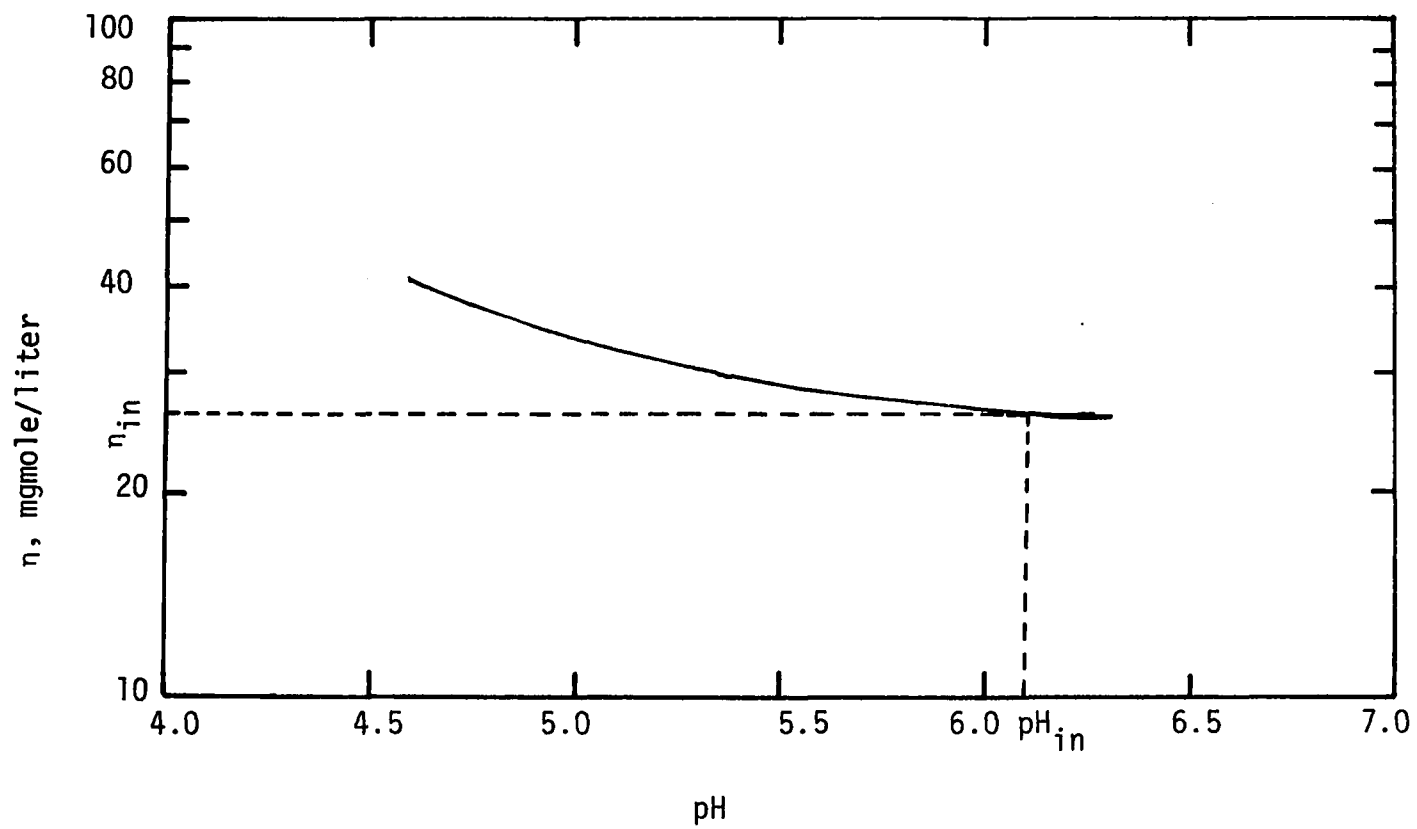


Figure A.1 Relationship Between η and pH for Lime Scrubbing System for the Example Given in Appendix B.

The agreement between the simulated and experimental values of pH and SO₂ removal efficiency appears fairly good.

Appendix B

Some Comments on the Concentration of Reactant, C_B , Calculated Via Equilibrium Computer Program

In order to utilize the equilibrium computer program (Nelson^[56], 1974), three major parameters must be specified. They are slurry pH, total sulfate concentration in the liquid phase and maximum CO_2 partial pressure. For limestone recycle slurry scrubbing system, an examination of the experimental data reveals that the variations of slurry pH and total sulfate concentration in the liquid phase across the scrubber are, in general, less than 15% (Borgwardt^{[10]~[21]}, 1972~1974). In addition, the maximum CO_2 partial pressure for the slurry in the scrubber appears most likely to be the flue gas CO_2 partial pressure. Thus, through an equilibrium calculation only a slight variation of concentration profile for each individual specie across the scrubber can be expected.

Examining the concentration of total carbonate in the liquid phase obtained from the equilibrium calculation and the experimental observation, it is shown that a reasonable agreement can be achieved. HCO_3^- which is identified as the major reactant specie contributes significantly towards the total carbonate concentration in the liquid phase. Consequently, it appears that the concentration of HCO_3^- can be approximated from an equilibrium calculation.

It is concluded that only a slight variation of concentration for the total carbonate in the liquid phase across the scrubber exists. The major reactant specie, HCO_3^- , can be approximated from the equilibrium calculation. The use of the inlet slurry condition specified

for the equilibrium calculation shown in this study offers convenient methods in determining the concentrations of reactant species via equilibrium calculation. (also see page 40 for reasons for using inlet slurry pH in the correlation of mass transfer coefficient).

TECHNICAL REPORT DATA (Please read Instructions on the reverse before completing)			
1. REPORT NO. EPA-600/2-75-023		3. RECIPIENT'S ACCESSION NO.	
4. TITLE AND SUBTITLE Absorption of Sulfur Dioxide in Spray Column and Turbulent Contacting Absorbers		5. REPORT DATE August 1975	
7. AUTHOR(S) C. Y. Wen and L. S. Fan		6. PERFORMING ORGANIZATION CODE	
9. PERFORMING ORGANIZATION NAME AND ADDRESS West Virginia University Department of Chemical Engineering Morgantown, West Virginia 26506		8. PERFORMING ORGANIZATION REPORT NO.	
12. SPONSORING AGENCY NAME AND ADDRESS EPA, Office of Research and Development Industrial Environmental Research Laboratory Research Triangle Park, NC 27711		10. PROGRAM ELEMENT NO. LAB013; ROAP 21ACY-041	
		11. CONTRACT/GRANT NO. Grant R-800781	
		13. TYPE OF REPORT AND PERIOD COVERED Final; 6/74 - 6/75	
		14. SPONSORING AGENCY CODE	
15. SUPPLEMENTARY NOTES			
16. ABSTRACT The report gives results of an analysis of experimental data, from both small and large scale turbulent contacting absorbers (TCA) and spray columns used in the wet scrubbing of SO ₂ from flue gases, to obtain gas film mass transfer coefficients and overall coefficients in the liquid film which includes chemical reaction in the liquid film. Recycled limestone, limestone-magnesium oxide, and lime scrubbing slurries were investigated. Gas film coefficients for the spray and TCA scrubbers were calculated from data on SO ₂ scrubbing with sodium carbonate solutions. Overall mass transfer resistances in the liquid phase were correlated for both scrubbers in terms of the ratio of the gas film and liquid film mass transfer resistances. The ratio of the resistances was found to be a function of only the scrubber type, inlet SO ₂ partial pressure in the gas phase, slurry pH, and magnesium concentration of the scrubbing slurry. Specifically, it was found that the ratio of the gas and liquid film mass transfer resistances (or the fraction to which SO ₂ removal is gas film controlled) increases with increasing slurry pH and magnesium concentration and decreasing SO ₂ partial pressure. Correlations for the gas film mass transfer coefficient and the ratio of mass transfer resistances are shown to predict fairly accurately the experimentally observed SO ₂ removal efficiencies.			
17. KEY WORDS AND DOCUMENT ANALYSIS			
a. DESCRIPTORS		b. IDENTIFIERS/OPEN ENDED TERMS	c. COSATI Field/Group
Air Pollution		Air Pollution Control	13B
Sulfur Dioxide		Stationary Sources	07B 11G
Absorption		Turbulent Contacting	11F
Calcium Oxides		Absorbers (TCA)	21B
Limestone		Spray Towers	07A, 07D
Magnesium Oxides			12A
Calcium Carbonates			
18. DISTRIBUTION STATEMENT Unlimited		19. SECURITY CLASS (This Report) Unclassified	21. NO. OF PAGES 114
		20. SECURITY CLASS (This page) Unclassified	22. PRICE